



**Universidade do Minho**  
Escola de Medicina

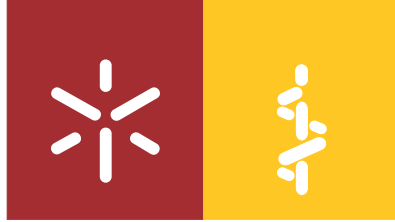
Inês Miguel Marques Pereira

## **Striatal modulation by lipocalin-2**

Inês Miguel Marques Pereira **Striatal modulation by lipocalin-2**

UMinho | 2018

maio de 2018



**Universidade do Minho**  
Escola de Medicina

Inês Miguel Marques Pereira

## **Striatal modulation by lipocalin-2**

Dissertação de Mestrado  
Mestrado em Ciências da Saúde

Trabalho efetuado sob a orientação da  
**Doutora Fernanda Marques**  
e da  
**Doutora Patrícia Monteiro**

*“Remember to look up at the stars and not down at your feet. Try to make sense of what you see and wonder about what makes the universe exist. Be curious. And however difficult life may seem, there is always something you can do and succeed at. It matters that you don't just give up.”*

*Stephen Hawking*



## AGRADECIMENTOS

**Embora todo o trabalho científico desenvolvido ao longo destes últimos meses, esta dissertação só foi possível pela presença e apoio de todos que estiveram comigo.**

Antes de mais, tenho que agradecer a ti Fernanda, obrigada por estes meses de orientação na minha introdução neste mundo das neurociências. Obrigada, primeiro, por me teres aceite e integrado nesta aventura e depois, por me teres ensinado e ajudado, sempre.

A ti Patrícia, obrigada pelas discussões científicas (sem esquecer dos lenços, claro), sem dúvida que foste uma parte fundamental no desenvolvimento desta tese. Obrigada pela tua boa-disposição e positivismo.

À Sofia, por me teres ensinado de tudo um pouco, desde da bancada até aos piqueniques no “Gerês”. Obrigada Sofia, foste um apoio fundamental e fico-te a dever uma!

Ao João, mais do que um tutor um amigo, obrigada por me teres ajudado em todos os momentos bons e menos bons! Obrigada por todos os conselhos e apoio ao longo destes dois anos!

Ao meu gang, Dani, Vero e Saró, obrigada por me terem recebido aqui tão bem, por me terem apoiado e estarem lá quando as coisas apertavam. Gosto muito de vocês e tenho a certeza que vão ainda rockar muito aqui pelo ICVS (ou afins).

À Beatriz, minha amiga de Aveiro, talvez que Aveiro não me deu, mas emprestou-me para eu trazer para Braga. Five stars for you! Começando pelos cafés, discussões científicas e não tanto científicas, pelas lágrimas, mas principalmente pelos risos e alegria, obrigada miúda!

À melhor mesa do ICVS, Diana, Rui e Margarida, que teria sido de mim sem vos aturar todos os dias? Sem todo o cacau que consumimos juntos? Obrigada por todos os momentos de filosofia proporcionados, pelas consultas grátis de psicologia, obrigada pelos deliciosos repastos e todos os bons momentos que passei convosco!

A todos os Nerd's que de uma forma ou outra tanto contribuíram para o desenvolvimento científico desta tese, como a nível pessoal.

Às minhas bffs, Rita e Neves, que lá de longe me vão aturando, me ouviram tanto a falar dos meus ratinhos sem nunca reclamarem (muito). Que nos momentos menos bons, foram as primeiras. Falar para quê?

Ao Miguel, que desde o início desta nova etapa da minha vida tens sido essencial. Tanto para me abrires os olhos, como para me amparares. Embora reclamasses o teu apoio foi incondicional. Obrigada por compreenderes as minhas ausências e por aproveitares as presenças. Obrigada!

Aos meus pais e ao meu irmão, que sempre foram e sempre serão o meu grande pilar! Que nunca questionaram as minhas ausências em casa e que sempre tentaram estar o mais presente possível, ao meu lado! Ao meu macaquinho, à minha estrelinha da sorte, que sempre iluminou e continua a iluminar a minha vida. À minha mãe, sinónimo de amor; e ao meu pai, sinónimo de preocupação. O meu maior obrigado!

The work presented in this thesis was performed in the Life and Health Sciences Research Institute (ICVS), Minho University. Financial support was provided from project NORTE-01-0145-FEDER-000013, supported by the Northern Portugal Regional Operational Programme (NORTE 2020), under the Portugal 2020 Partnership Agreement, through the European Regional Development Fund (FEDER), and funded by FEDER funds through the Competitiveness Factors Operational Programme (COMPETE), and by National funds, through the Foundation for Science and Technology (FCT), under the scope of the project POCI-01-0145-FEDER-007038.







## ABSTRACT

Lipocalin-2 (LCN2) was first described as an acute-phase molecule involved in the innate immune response against several pathological stimuli. However, recent studies have also associated LCN2 as an important mediator in the central nervous system (CNS) physiology. Noteworthy, it was recently shown that peripheral LCN2 is a new ligand of the melanocortin 4 receptor (MC4R) and that, by binding to this receptor in the hypothalamus, LCN2 can suppress food intake, which is considered a type of compulsive behavior. Of interest, it was shown that both constitutive and induced genetic deletion of the gene encoding MC4R, as well as the pharmacological inhibition of MC4R signaling, normalized compulsive grooming and striatal electrophysiology impairments in synapse-associated protein 90/postsynaptic density protein 95-associated protein 3 (SAPAP3)-null mice, a model of human obsessive-compulsive disorder (OCD). However, in this report, it was not clear the mechanisms through which MC4R deletion leads to the rescue of the phenotype. One possibility is that the ligands for MC4R are no longer inducing its effects once the receptor is deleted. This is especially relevant after the demonstration that MC4R agonists induced compulsive grooming in wild-type mice and in rats. Thus, we hypothesize that the mechanism through which MC4R deletion leads to phenotypic rescue of SAPAP3-null mice can be by LCN2 signaling.

For that reason, herein, we took advantage of a mouse strain with a target deletion of the *Lcn2* gene (LCN2-null mice), we analyzed the role of LCN2 in the striatum through electrophysiological, morphological, behavioral and cellular approaches. Overall, our findings showed that LCN2-null mice have altered striatal excitatory transmission, implicating the same brain region that has been reported in SAPAP3-null mice. Concomitantly, behavioral approaches showed that LCN2-null mice displayed an excessive burying response and a habitual behavior in an operant conditioning test that is highly regulated by the dorsolateral striatum (DLS). Regarding molecular analysis, we showed that LCN2 ablation leads to an increase in *Psd-95* expression. Altogether, a possible novel role for LCN2 in the striatal modulation, not only at the synaptic level but also in morphological and molecular mechanisms, is suggested.



## RESUMO

A lipocalina-2 (LCN2) foi inicialmente descrita como sendo uma proteína de fase aguda envolvida em respostas da imunidade inata contra vários estímulos patológicos. No entanto, estudos recentes associam a LCN2 como um importante mediador no sistema nervoso central. Recentemente, foi mostrado que a LCN2 é um novo ligante para o recetor melanocortina 4 (MC4R) e que, no hipotálamo, tem um efeito supressor da ingestão de alimentos, considerado um tipo de comportamento compulsivo. Além disto, foi demonstrado que a deleção genética do gene que codifica o recetor MC4R, bem como a inibição farmacológica da sua sinalização, normaliza o comportamento compulsivo e a eletrofisiologia do estriado de ratinhos que não expressam a proteína associada à sinapse 90 / densidade pós-sináptica Proteína 95 associada a proteína 3 (SAPAP3), um modelo animal de perturbação obsessiva compulsiva (POC) humano. No entanto, neste estudo, não ficou claro os mecanismos pelos quais a deleção do MC4R leva ao resgate do fenótipo. Uma possibilidade é que os ligantes do recetor MC4R não estejam mais a induzir os seus efeitos uma vez que este se encontra deletado.

Assim, levantamos a hipótese que o mecanismo pelo qual a deleção do MC4R leva ao resgate fenotípico de ratinhos sem expressão da proteína SAPAP3 seja pela sinalização da LCN2. Tirando vantagem de um modelo de ratinho no qual o gene que codifica *Lcn2* foi removido, analisamos o impacto desta no estriado através de abordagens eletrofisiológicas, morfológicas, comportamentais e celulares. No geral, os nossos resultados demonstram que ratinhos que não expressam LCN2 apresentam uma alteração da transmissão excitatória do estriado, na mesma região que foi descrita em ratinhos modelo de POC (SAPAP3-null). Concomitantemente, a não expressão da LCN2 induz uma alteração no comportamento destes animais. De facto, os animais nos quais o gene *Lcn2* foi removido demonstram uma resposta excessiva de “burying” e um comportamento habitual quando submetidos a um teste de condicionamento operante. Em relação à análise molecular, mostramos que a não expressão de LCN2 leva a um aumento na expressão do gene *Psd-95*. Em conjunto, sugerimos um possível novo papel para a LCN2 na modulação do estriado, não apenas a nível sináptico, mas também nos mecanismos morfológicos e moleculares.



# TABLE OF CONTENTS

Agradecimientos.....	v
Abstract.....	ix
Resumo .....	xi
Table of Contents .....	xiii
Figures Index .....	xv
Tables Index .....	xvii
List of Abbreviations.....	xix
<b>1. INTRODUCTION .....</b>	<b>1</b>
<b>1.1 LIPOCALIN-2 .....</b>	<b>3</b>
<b>1.1.1 Functions .....</b>	<b>3</b>
1.1.1.1 Involvement of LCN2 in immunity.....	5
1.1.1.2 LCN2 and iron homeostasis.....	6
<b>1.1.2 LCN2 receptors.....</b>	<b>7</b>
<b>1.1.3 LCN2 in the Central Nervous System.....</b>	<b>9</b>
<b>1.2 OBSESSIVE-COMPULSIVE DISORDER .....</b>	<b>13</b>
<b>1.2.1 Obsessive-compulsive disorder: an overview.....</b>	<b>13</b>
<b>1.2.2 Melanocortin 4 receptor as an indirect modulator of compulsive behaviors .....</b>	<b>14</b>
<b>1.2.3 The role of the cortico-striato-thalamocortical circuitry.....</b>	<b>16</b>
<b>1.3 STRIATUM .....</b>	<b>18</b>
<b>1.3.1 An overview.....</b>	<b>18</b>
<b>1.3.2 The role of striatum in Decision-Making .....</b>	<b>19</b>
<b>1.3.3 Neuronal striatal cells .....</b>	<b>21</b>
<b>2. AIMS.....</b>	<b>23</b>
<b>3. MATERIAL AND METHODS.....</b>	<b>27</b>
<b>3.1 Experimental Animals.....</b>	<b>29</b>
<b>3.2 Genotyping.....</b>	<b>30</b>
<b>3.3 Behavioral procedures.....</b>	<b>32</b>
3.3.1 Operant conditioning test.....	32
3.3.2 Marble burying test .....	35
<b>3.4 Golgi-Cox staining .....</b>	<b>35</b>

<b>3.5</b>	<b><i>Structural dendritic tree analysis</i></b> .....	<b>36</b>
<b>3.6</b>	<b><i>Gene expression analysis</i></b> .....	<b>38</b>
3.6.1	RNA extraction and quantification .....	38
3.6.2	DNase/RNase-free treatment .....	38
3.6.3	Complementary DNA (cDNA) synthesis.....	39
3.6.4	Quantitative Real-Time PCR (qRT-PCR) gene expression analysis.....	39
<b>3.7</b>	<b><i>Slice electrophysiology</i></b> .....	<b>40</b>
<b>3.8</b>	<b><i>Statistical analysis</i></b> .....	<b>43</b>
<b>4.</b>	<b>RESULTS</b> .....	<b>45</b>
<b>4.1</b>	<b><i>Decision-making is biased in the absence of LCN2</i></b> .....	<b>47</b>
<b>4.2</b>	<b><i>LCN2-null mice present excessive marble burying behavior</i></b> .....	<b>49</b>
<b>4.3</b>	<b><i>Medium spiny neurons at the dorsomedial striatum are atrophic in the absence of LCN2</i></b> . 51	
<b>4.4</b>	<b><i>Dorsomedial striatum neurons have lower amplitude of synaptic transmission in the absence of LCN2</i></b> .....	<b>54</b>
<b>4.5</b>	<b><i>Dorsomedial striatum neurons have lower amplitude of synaptic transmission in naïve LCN2-null mice</i></b> . .....	<b>55</b>
<b>4.6</b>	<b><i>The absence of LCN2 induces increased Psd-95 gene expression</i></b> .....	<b>58</b>
<b>5.</b>	<b>DISCUSSION</b> .....	<b>61</b>
<b>6.</b>	<b>FINAL REMARKS</b> .....	<b>69</b>
<b>7.</b>	<b>REFERENCES</b> .....	<b>73</b>

## Figures Index

<b>Figure 1</b>	The bone-brain axis suggested by Mosialou <i>et al.</i> in modulating food intake.	Page 11
<b>Figure 2</b>	The basis of the obsessive-compulsive behavior <i>loop</i> as a multidimensional disorder.	Page 13
<b>Figure 3</b>	Comparative compulsive outcome in different genetic mice.	Page 16
<b>Figure 4</b>	The cortico-striato-thalamocortical circuitry comparing OCD patients to healthy individuals.	Page 17
<b>Figure 5</b>	Neuroanatomic differences between the cortico-striatal circuitry in humans (A) and mice (B) brains.	Page 19
<b>Figure 6</b>	Medial-lateral functional gradient of the dorsal striatum that are underlying goal-directed and habitual action strategies.	Page 20
<b>Figure 7</b>	Schematic diagram of the theoretical hypothesis proposed for this thesis.	Page 26
<b>Figure 8</b>	LCN2-null mice model.	Page 29
<b>Figure 9</b>	Colony management strategy to maintain LCN2-null mice and WT littermate controls phenotype.	Page 30
<b>Figure 10</b>	Schematic representation of the genotype strategy used to identify LCN2-null mice	Page 31
<b>Figure 11</b>	Schematic representation of the operant task.	Page 34
<b>Figure 12</b>	Spine morphology classification	Page 37
<b>Figure 13</b>	LCN2-null mice presented a habitual lever pressing behavior when compared to the control group in an operant task.	Page 49
<b>Figure 14</b>	LCN2-null mice display a compulsive and anxious phenotype in the marble burying test.	Page 50
<b>Figure 15</b>	Three-dimensional morphological analysis of Golgi-impregnated medium spine neurons (MSNs), of the dorsomedial (DMS) and dorsolateral striatum (DLS) reveals no major alterations by the absence of LCN2.	Page 53

<b>Figure 16</b>	Synaptic pattern in LCN2-null mice is not altered after behavioral tests in dorsomedial striatum medium spiny neurons.	Page 55
<b>Figure 17</b>	LCN2-null mice displayed reduced amplitude of excitatory synaptic transmission in dorsomedial striatum medium spiny neurons.	Page 57
<b>Figure 18</b>	LCN2 absence does not induce major differences in striatal gene expression.	Page 59
<b>Figure 19</b>	Differential expression of specific gene markers in the striatum.	Page 60
<b>Figure 20</b>	Schematic overview of the observed LCN2-null mice phenotype.	Page 65
<b>Figure 21</b>	Hypothetical role for LCN2 in the involvement of OCD-like behaviors.	Page 66



## Tables Index

<b>Table 1</b>	Primer sequences for the polymerase chain reaction (PCR).	Page 31
<b>Table 2</b>	PCR Mix components and PCR conditions for genotyping strategy.	Page 32
<b>Table 3</b>	Primers sequences used to determine the relative expression of a target gene using the qRT-PCR method.	Page 40
<b>Table 4</b>	Solution reagents list used during the slice electrophysiological protocol.	Page 42
<b>Table 5</b>	Statistical analysis performed during the instrumental task, both during training and devaluation test in LCN2-null mice and littermate controls.	Page 48
<b>Table 6</b>	Statistical analysis of the marble burying test.	Page 50
<b>Table 7</b>	Statistical results of the morphological analysis comparing LCN2-null with wild-type mice in both DMS and DLS areas.	Page 52
<b>Table 8</b>	Statistical analysis of electrophysiological recordings comparing LCN2-null mice with littermate controls.	Page 54
<b>Table 9</b>	Statistical analysis of electrophysiological recording comparing LCN2-null mice with littermate controls.	Page 56
<b>Table 10</b>	Statistical analysis regarding relative gene expression in the striatum.	Page 60



## List of Abbreviations

### A

**A2aR** A2a adenosine  
**ACh** Acetylcholine  
**aCSF** Artificial cerebrospinal fluid  
**ACTH** Adrenocorticotrophic hormone  
**AMPA**  $\alpha$ -amino-3-hydroxy-5-methyl-4-isoxazolepropionic acid

### B

**BBB** Blood-brain barrier

### C

**cDNA** Complementary DNA  
**ChIs** Aspinic cholinergic interneurons  
**CNS** Central nervous system  
**CP** Choroid plexus  
**CSF** Cerebrospinal fluid  
**CSTC** Cortico-striato-thalamocortical circuitry

### D

**D1** Dopamine type 1  
**D1R** D1 receptor  
**D2** Dopamine type 2  
**D2R** D2 receptor  
**DA** Dopamine  
**DBS** Deep brain stimulation  
**DLS** Dorsolateral striatum  
**DMS** Dorsomedial striatum  
**DS** Dorsal striatum  
**DSM-5** Diagnostic and Statistical Manual of Mental Disorders

### F

**Fe<sup>3+</sup>** Ferric iron  
**FR-1** Fixed ratio 1

### G

**GABA** Gamma aminobutyric acid  
**GP** Globus pallidus  
**GPe** Globus pallidus externus

**GPI** Globus pallidus interna

### I

**IL** Infralimbic  
**IR-DIC** Infrared differential interference contrast

### L

**LCN2** Lipocalin-2  
**LPS** Lipopolysaccharide

### M

**MC4R** Melanocortin 4 receptor  
**MMP9** Metalloproteinase 9  
**mPFC** Medial prefrontal cortex  
**MSH** Melanocyte-stimulating hormone  
**MSNs** Medium spiny neurons  
**mEPSC** miniature excitatory postsynaptic currents

### N

**NAc** Nucleus accumbens  
**Neo** Neomycin  
**NGAL** Neutrophil gelatinase-associated lipocalin  
**NMDA** *N*-methyl-D-aspartate receptor

### O

**OCD** Obsessive-compulsive disorder  
**OFC** Orbitofrontal cortex

### P

**PCR** Polymerase chain reaction  
**PFC** Prefrontal cortex  
**PL** Prelimbic  
**PSD-95** Postsynaptic density protein 95  
**PVH** Paraventricular of hypothalamus

### Q

**qRT-PCR** Quantitative Real-Time PCR

**R****RR-10** Random Ratio 10**RR-20** Random Ration 20**RT** Room temperature**S****SAPAP3** Synapse-associated protein 90/postsynaptic density protein 95-associated protein 3**SNr** Substantia nigra pars reticulate**SSRIs** Selective serotonin reuptake inhibitors**STN** Subthalamic nucleus**STR** Striatum**Syp** Synaptophysin**T****Ta** Temperature of annealing**TLR** Toll-like receptor**TM** Temperature of melting**V****VMH** Ventromedial nucleus of hypothalamus**W****WT** Wild-type**Y****Y-BOCS** Yale-Brown Obsessive Compulsive Scale

## CHAPTER 1

---

### 1. INTRODUCTION



## 1.1 LIPOCALIN-2

### 1.1.1 Functions

Lipocalin-2 (LCN2) is a small secreted and soluble protein that belongs to the lipocalin superfamily, a vast number of molecules involved in health and disease processes (Flower et al., 1996). Members of this family are typically characterized based on their molecular properties, such as the ability to bind small molecules, specific cell-surface receptors and the capacity to form macro-molecular complexes (Flower et al., 1996). Lipocalins are a very large and diverse group of proteins, that vary within and between species, presenting a vast functional and structural diversity (Flower et al., 2000). In the past, the lipocalin family was simply described as a transport protein family. Nowadays, on the contrary, it is clearly accepted that lipocalin superfamily is involved in several important processes, including prostaglandin synthesis (Lim et al., 2013), cell homeostasis (division, differentiation, adhesion and survival) (Flower et al., 2000), immune response modulation (Flo et al., 2004) and transport (clearance of endogenous and exogenous molecules) (Bao et al., 2015; Flower et al., 2000). Hereupon, as a lipocalin family member, the transport protein LCN2 has also been remarkably described as an important molecule involved in a variety of physiological and pathophysiological processes.

Due to this described finding, throughout time, LCN2 (the formal designation by the HUGO Gene Nomenclature Committee) has also been known as 24p3, NGAL, oncogene 24p3, human neutrophil lipocalin,  $\alpha$ 2-microglobulin related protein, siderocalin and uterocalin. LCN2 (lipocalin product of a single gene, the *24p3*) was first identified in 1989 as an over-expressed gene in infected murine kidney cell culture (Hraba-Renevey et al., 1989). Then, LCN2 was identified in humans as a 25 kDa protein covalently linked to the 92 kDa metalloproteinase 9 (MMP-9) in neutrophils, being denominated as “neutrophil gelatinase-associated lipocalin” (NGAL) with no attributed functions (Kjeldsen et al., 1993; Triebel et al., 1992). Further, murine LCN2 was also identified as an acute-phase protein with an important role in immune response modulation (Liu & Nilsen-Hamilton, 1995).

In humans, NGAL (human ortholog of mouse *Lcn2* gene) was shown to be differentially expressed during the human embryonic development, in a spatio-temporal manner (Mallbris et al., 2002). In postnatal stages, NGAL levels strongly increase in healthy

tissues (Aigner et al., 2007) but during time, its expression declines (Garay-Rojas et al., 1996). Nevertheless, LCN2 has been identified in multiple tissues including liver, spleen, kidney (Aigner et al., 2007), bone marrow (Cowland & Borregaard, 1997) and white adipose tissue (Yan et al., 2007). Despite its broad expression, LCN2 is specially up-regulated in tissues that are more susceptible to infection, such as the mucosal (Kjeldsen et al., 2000) and epithelial barriers (Friedl et al., 1999), concomitant with its crucial bacteriostatic role against pathogenic microorganisms. Moreover, LCN2 is also secreted by a variety of cells such as neutrophils, adipocytes (Kjeldsen et al., 1993), leukocytes, peritoneal cells (Flo et al., 2004), macrophages (Meheus et al., 1993), chondrocytes (Owen et al., 2008) endothelial cells, choroid plexus (CP) epithelial cells (Marques et al., 2008) and astrocytes (Marques et al., 2012). Consequently, this pleiotropic molecule is involved in a series of mechanisms, such as: transport of fatty acids (Chu et al., 1998), iron metabolism (Yang et al., 2002), cellular apoptosis (Devireddy et al., 2001), inflammatory responses (Cowland & Borregaard, 1997), metabolic homeostasis (Yan et al., 2007), infection and immunity modulation (Li et al., 2018) and brain processes (*e.g.*: neurogenesis (Ferreira et al., 2018)).

To add, LCN2 over-expression can be triggered by many different factors and conditions including cytokines, growth factors, glucocorticoids, and lipopolysaccharide (LPS), being LPS the strongest one (Meheus et al., 1993). Specifically, it was demonstrated that LCN2 is highly expressed in macrophages after *in vitro* LPS stimulation (Meheus et al., 1993) and, *in vivo* experiments (Marques et al., 2008) had also shown an increase in LCN2 concentration after intraperitoneal LPS stimulation mediated via Toll-like receptor (TLR)-4 (Flo et al., 2004).

Altogether, LCN2 has emerged as a pleiotropic molecule with notable functions in the control, support or even in the disturbance of several homeostatic conditions. Thus, to a better comprehensive insight of the underlying impact, LCN2 functions will be further discuss in more detail.



#### 1.1.1.1 Involvement of LCN2 in immunity

Constantly, mammalian cells are faced with harmful and pathogenic microorganisms that attempt to enter into the host and take advantage of their nutrients/energy storage. Thus, the immunity of mammals is challenged to fight and resist to the bacterial burden (Nicholson et al., 2016).

Iron is crucial to bacterial proliferation (Caza et al., 2013; Parrow et al., 2013). Relying on these, host mammalian cells have developed a variety of defense mechanisms that consist basically in decreasing iron availability and therefore inhibiting bacterial survival. However, natural selection and adaptation led several microorganisms to engage new strategies to overcome poor-iron environments, such as iron-binding siderophores (Miethke & Marahiel, 2007). These are small molecules secreted by bacteria that have higher affinity to iron when compared to host iron carriers, thus sequestering iron from the host's protein-iron complexes (Neilands et al., 1995).

Noteworthy, it was shown *in vitro* that LCN2 has a high affinity for bacterial siderophores, both in their iron-loaded and iron-free states, and that it even competes with the pathogen for iron, in order to limit bacteria propagation (Goetz et al., 2002). Upon this discovery, LCN2 was immediately suggested to be involved in the innate immunity as a bacteriostatic iron-sequestering molecule. At the time, Goetz *et al.* (2002), assumed that LCN2 was released by neutrophils at sites of infection to preclude bacterial iron acquisition, thus participating in the antibacterial iron-depletion strategy of the innate immune response (Goetz et al., 2002). We now know that LCN2 is a potent bacteriostatic agent that acts as a chelator of bacterial siderophores, being released from liver and spleen, among other tissues, after an infection (Flo et al., 2004). However, LCN2 effect is limited to the catecholate-type siderophores, which represents a limitation, since different bacteria release different siderophores (Holmes et al., 2005).

Unexpectedly, in 2010, Bao and his colleagues reported the existence of an endogenous mammalian siderophore (Bao et al., 2010), suggesting new roles for LCN2 as an important molecule in physiologic conditions and, more specifically in iron-trafficking homeostasis. Briefly, the identified mammalian siderophore is a small catechol that by itself binds poorly to the LCN2, but when ferric iron ( $\text{Fe}^{3+}$ ) is present the affinity between

them improves significantly (Bao et al., 2010). Moreover, mammalian siderophore features appear to be conserved from bacteria to mammalian, based on iron-binding moiety similarities and their synthesis mechanism that seems to be homologue to the bacterial production (Devireddy et al., 2010). Once they are very similar, bacterial pathogens have also the ability to take advantage of mammalian siderophores and rescue iron from the mammalian host. Nevertheless, contradicting it, infected hosts developed a strategy to inhibit the production of the enzyme responsible for the formation of mammalian siderophores in the presence of a bacterial pathogen (Devireddy et al., 2010).

Moreover, it was recently described that LCN2 was up-regulated in different cell types, that are involved in the combat and control of bacterial infection (Li et al., 2018). For instance, after local *Klebsiella pneumoniae* infection Li *et al.* (2018) demonstrated that, hepatocytes secrete LCN2 to control systemic infection, while neutrophils are more involved in carrying LCN2 to attenuate the infection *in loco*.

Overall, the pleiotropic LCN2 protein represents a crucial immunologic mediator in the immune system highly involved in the first line of defense. In addition, the existence of a mammalian siderophore has also brought new promising insight into the field, mainly regarding the role of LCN2 as a potential iron regulator in homeostatic conditions.

#### 1.1.1.2 LCN2 and iron homeostasis

Iron is an essential metal mostly intracellularly that binds to the complex ferritin protein (Arosio et al., 2017) and it is a crucial element in enzymes, cytochromes and protein prosthetic groups. As so, iron is involved in many physiologic processes, such as oxygen transport, cell proliferation and differentiation, and even in cell death and metabolism (Arosio et al., 2017). Moreover, systemic iron imbalances have severe repercussions that may lead to the development of critical pathological conditions (Moreno-Navarrete et al., 2017), whether by iron excess [*e.g.*: hemochromatosis (Adams et al., 2015)] or deficiency [*e.g.*: anemia (Camaschella, 2015)]. Also iron deposition is related with the pathology and progression of some neurodegenerative disorders, such as Parkinson's and Alzheimer's disease (Yien & Paw, 2016).

So far, no specific mechanism has been described for iron excretion, apart from bleeding and skin and enterocyte renewal (Saito et al., 2014). In consequence, iron levels in the body are mainly controlled at the absorption level. The liver is the main responsible for this balance, since it is able to produce hepcidin (Kim & Nemeth, 2015), when the levels of this metal are elevated. Briefly, hepcidin is able to bind in the basolateral side of enterocytes to ferroportin (the iron export transporter), thus blocking iron release from the enterocytes to the bloodstream. Once in the bloodstream, iron is traditionally described to be transported by transferrin, being acquired by different body cells through a receptor-mediated endocytosis of iron-loaded transferrin (Arosio et al., 2017).

Until very recently, transferrin was the only recognized protein able to delivery iron to cells. However, a novel role for LCN2 has been emerging, as a putative molecule involved on iron trafficking. As already mentioned, LCN2, even in the absence of bacterial infection, is able to interact with iron through the recently described endogenous mammalian catechol complex (Bao et al., 2010). Thus, the existence of an LCN2-mediated iron-delivery pathway has been supported and suggested by different studies. In accordance, it was also demonstrated that LCN2 iron-delivery is very important in epithelial cell differentiation, during the development of mammalian kidney (Yang et al., 2002). Therefore, LCN2 is a promising molecule in the regulation of homeostatic iron trafficking. Supporting these insights, it is also known that transferrin is only expressed at advanced stages of organogenesis, reinforcing the existence of other molecules to provide iron in earlier developmental stages (Gustine & Zimmermant, 1973).

Altogether, and considering the studies reported by Bao *et al.* (2010) and Devireddy *et al.* (2010) regarding the mammalian endogenous siderophore (Bao et al., 2010; Devireddy et al., 2010), LCN2 has been considered as an iron import and/or export protein through a transferrin-independent mechanism.

### **1.1.2 LCN2 receptors**

Several receptor for LCN2 have been described. In 2005 Hvidberg and his colleagues firstly demonstrated megalin as a LCN2 endocytic receptor involved its cellular uptake (Hvidberg et al., 2005). In the same year, the solute carrier family 22 (organic cation

transporter) member 17 (SLC22A17), commonly named as 24p3R, was also revealed and isolated as an elegant LCN2 receptor for iron transport (Devireddy et al., 2005).

Megalin is a multi-ligand endocytic receptor expressed in epithelia that is also known to bind, among others, to the  $\alpha$ 2-microglobulin and mouse lipocalin retinol-binding proteins (Christensen & Birn, 2002). In Hvidberg's work, it was reported that both iron-lacking-LCN2 (apo-LCN2) and iron-loaded-LCN2 (holo-LCN2) were able to bind megalin, allowing LCN2 endocytosis (Hvidberg et al., 2005). The affinity of megalin to bind and internalize LCN2 was confirmed by concomitant tissue expression this receptor after induction of LCN2 expression during inflammation (Hvidberg et al., 2005). Interestingly, in the same year, 24p3R was also demonstrated to be able to internalize LCN2 whether in its apo- or holo-forms (Devireddy et al., 2005). In this sense, it is capable of modulating iron metabolism by facilitating its uptake and excretion through a specific mechanism highly dependent on the LCN2 form-ligand. Briefly, holo-LCN2 binds to 24p3R forming endosomes, and release the bound-iron in the cellular cytoplasm leading to an increase intracellular iron concentration, which seems to be related with decreased apoptosis. On the contrary, apo-LCN2 internalization chelates iron intracellularly and allocates it to the extracellular medium, leading to an iron efflux (Devireddy et al., 2005). Expectedly, the reduction of intracellular iron concentrations results in cell death, which is described to be mediated and stimulated by the pro-apoptotic Bcl-2-interacting mediator of apoptosis (Bim) (Devireddy et al., 2005).

Surprisingly, Mosialou *et al.* (2017) have recently identified a novel LCN2 receptor the melanocortin 4 receptor (MC4R). MC4R is a well-described G-protein coupled receptor, mainly expressed in the brain. By *in situ* hybridization MC4R mRNA was localized preferentially in regions of the thalamus, hypothalamus, and hippocampus (Gantz et al., 1993). Functionally, MC4R has been described as a critical molecule involved in food intake regulation, body weight, caloric efficiency (Adan et al., 2006; Pandit et al., 2015) and even in pain regulation (Li et al., 2017). Regarding Mosialou's work, he was interested in investigating how food intake behavior is controlled at the molecular level in the brain (Mosialou et al., 2017). Outstandingly, they have found that the peripheral LCN2 is able to bind specifically to MC4R in the paraventricular (PVH) and ventromedial nucleus (VMH) of the hypothalamus. As it is illustrated further in Figure 1, after the

interaction between these two molecules neuronal activation leads to food intake suppression (Mosialou et al., 2017).

Considering these novel insights and other relevant reports (Ferreira et al., 2013; Ferreira et al., 2018), a critical role for LCN2 has emerged in the control of central nervous system (CNS) homeostasis. These considerations open and support new opportunities to LCN2 in the scope of brain functioning.

### 1.1.3 LCN2 in the Central Nervous System

In the CNS, recent and important roles for LCN2 in brain homeostasis have been pointed out. A first report has shown LCN2 expression in the whole brain after an inflammatory stimuli (Liu & Nilsen-Hamilton, 1995), then in mouse brain after local ischemia (MacManus et al., 2004) and in spinal cord injury (De Biase et al., 2005; Poh et al., 2012). Meanwhile, it was demonstrated that LCN2 up-regulation was present in diverse pathological conditions including peripheral inflammatory stimulation (Marques et al., 2008), Alzheimer's disease (Mesquita et al., 2014) and Multiple Sclerosis (Marques et al., 2012). Although it is well accepted that LCN2 is highly expressed in the brain when an insult or injury is imposed (Ferreira et al., 2015), an intense debate regarding the possible production of LCN2 under basal conditions is still present. Indeed, in the adult rat brain, LCN2 was reported to be expressed in most brain regions at low levels but in the olfactory bulb, brainstem and cerebellum its expression levels were higher (Chia et al., 2011). However, a considerable number of reports showed that LCN2 is absent in the basal physiological brain and its levels were below the detection range in the cerebrospinal fluid (CSF) of non-stimulated mice (Marques et al., 2008). Also, other area of debate is related, which cells in the CNS are able to produce LCN2. In the Chia *et al.*, (2011) study, LCN2 expression in basal conditions seems to be limited to astrocytes (Chia et al., 2011), while Mucha *et al.* (2011), has also shown that hippocampal neurons were able to produce LCN2, even in physiological conditions (Mucha et al., 2011). Noticeably, also the precise identification of the brain cells that are able to produce LCN2 in response to injury is an interesting question and represents a second level of controversy in the field.

Despite such controversy, more recently the role of LCN2, whether produced in the periphery or admitting its local production at the brain, in the normal brain physiology has been extensively studied. Of interest, using a genetic mice model with ablation of *Lcn2* expression (LCN2-null mice) it was shown an increase on anxiety and depressive-like behavior and impairments in spatial reference memory (Ferreira et al., 2013). Behavioral manifestations were associated with significant alterations in the morphology and spine density of hippocampal neurons along the dorsal-ventral axis (Ferreira et al., 2013). While in ventral hippocampus it was shown a neuronal hypertrophy, in the dorsal division neurons were atrophic in the absence of LCN2 (Ferreira et al., 2013). Still, it was also demonstrated that LCN2-null mice present an increased stress response, which was correlated with a higher excitability of CA1 neurons and stress-induced anxiety (Mucha et al., 2011). Along with roles in brain homeostasis, LCN2 was also shown to be involved in adult neurogenesis, differentiation and survival (Ferreira et al., 2018). Hence, such alterations resulted in behavioral impairments of hippocampal-dependent contextual fear discriminative activity (Ferreira et al., 2018).

Overall, along these topics, LCN2 has been described as an important regulator of brain processes; however, always with some controversy associated. Exceptionally, it is clear the role of this acute-phase protein in avoiding the malfunctioning of biologic systems, particularly in the brain. As an additional example, and of relevance in the context of the present thesis, is the work of Mosialou *et al.*, (2017). In this work, the authors revealed that peripheral LCN2, produced by osteoblasts (bone-forming cells) in a nutrient-sensitive manner, was able to stimulate specific receptors on hypothalamic neurons and, consequently, to suppresses appetite (Mosialou et al., 2017). It was demonstrated that mice that could not produce LCN2 specifically in osteoblasts had increased level of food intake, gained more weight, and showed impaired capacity to metabolize glucose. Further, the authors also showed the same traits in LCN2-null mice, sustaining the fact that LCN2 acts as a hormone to reduce appetite (Mosialou et al., 2017). Since the feeding behavior is controlled by the brain, the next plausible step followed by the authors was to measure the amount of LCN2 in the brain and identify the receptor protein responsible for LCN2-induced anorexia. Thus, Mosialou *et al.* (2017) showed that LCN2 crosses the blood-brain barrier (BBB), binds to MC4R in the PVH and VMH neurons and activates a MC4R-dependent anorexigenic (appetite-suppressing) pathway (Figure 1) (Mosialou et

al., 2017). Moreover, people with MC4R mutation are often obese and presented elevated LCN2 blood levels when compared to weight-matched people without the mutation (Farooqi & O'Rahilly, 2008). These studies are relevant in the context of the present thesis for two different reasons: it links LCN2 to a compulsive behavior, that is food consumption, and it links LCN2 to MC4R that, as we will discuss later, is also linked with compulsive behaviors.

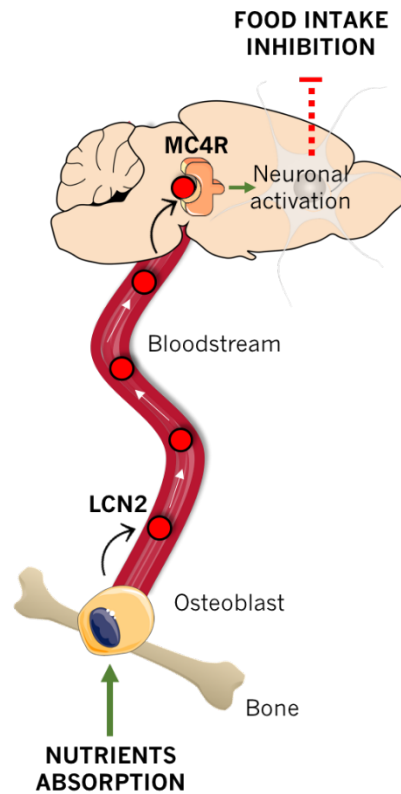


**Figure 1: The bone-brain axis suggested by Mosialou et al. in food intake modulation.** Lipocalin-2 released by bone-forming cells (osteoblasts) after nutrients absorption enters in circulation until it reaches the hypothalamus, where it binds to the melanocortin 4 receptor (MC4R) on neurons. Consequently, neuronal activation leads to the induction of a signaling pathway that suppresses food intake.

As mentioned before, in addition to the well-known role of MC4R in the hypothalamus for feeding control and energy expenditure (Balthasar et al., 2005), it has also been recently shown that MC4R operates within dopamine type 1 (D1) medium spiny neurons (MSNs) at the ventral striatum to mediate procedural memory and affective response to stress (Cui et al., 2012; Lim et al., 2012). Moreover, previous reports have suggested that stimulation of MC4R-signaling induces compulsive grooming in rats (Alvaro et al., 2003).

These finding, linking LCN2 to MC4R and, in turn, MC4R to compulsive behaviors, are relevant in the context of the present thesis. Altogether, this points to a new putative role for LCN2, relating its new brain receptor (MC4R) and its involvement in obsessive-compulsive behaviors, which are regulated by MSNs at the striatum. Therefore, in the next sections, the neurobiological pathways involved in obsessive-compulsive disorder (OCD) will be further described, to better understand all the dimensions of the disease both at clinical and molecular levels.



## 1.2 OBSESSIVE-COMPULSIVE DISORDER

### 1.2.1 Obsessive-compulsive disorder: an overview

OCD is a relatively common neurodevelopmental disorder with a prevalence rate of 2-3% worldwide (APA, 2013). This early-onset neuropsychiatric condition varies among patients with a wide range of symptomatic expression. The age of onset ranges from very early childhood (30-50%; often before 10 years old) into adulthood (Boedhoe et al., 2017; Fogel, 2003).

OCD diagnosis and characterization are very complex processes and disease severity tends to increase throughout life. It is a long-lasting disorder in which a person has uncontrollable, reoccurring thoughts (obsessions) and behaviors (compulsions). Obsessions are persistent, excessive preoccupations with uncontrollable thoughts, images, or impulses that remain constant, unwanted and cause anxiety and discomfort, interfering with patients' routines. Compulsions are specific and repetitive rituals/behaviors that are performed according to specific rules, attempting to extinguish the anxiety caused by the obsessions. These repetitive behaviors, may or not have a minimum impact in releasing the distressed felt by the obsession, but at least temporarily it allows a relief sensation, as it is demonstrated in Figure 2 (Nestadt et al., 2011).

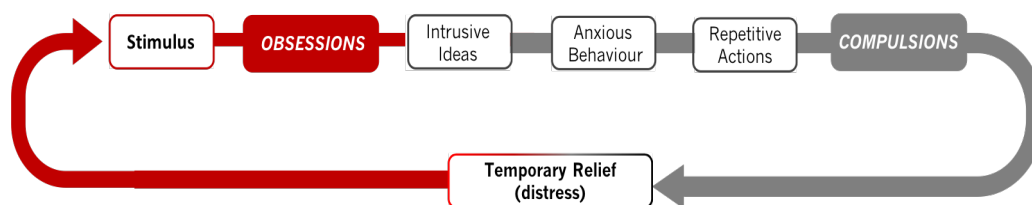


**Figure 2: The basis of the obsessive-compulsive behavior loop as a multidimensional disorder.** People with OCD live in a mental loop where a specific stimulus, external or internal, drive in them consistent thoughts, or images (obsessions), which are associated with a high level of anxiety and distress. In an attempt to neutralize these feelings, the patients perform ritualized and repetitive behaviors (compulsions). Although, these actions provide a temporary relief, they lead to a reinforcement of the compulsions. Overall, OCD is a very complex and multidimensional disorder.

There is a plethora of possible stimulus that might be the triggering cause on OCD patients, for instance, the increased fear of being contaminated with dirt or germs by touching. In this case, the thought of touching causes a lot of anxiety (obsession) to the individual that tries to overcome it by hand-washing. However, the cleaning is not a satisfactory action, and the individual keeps washing excessively, sometimes until hands are raw and/or

bleeding (compulsion). Once this action seems to be concluded, the individual has a temporary relieving feeling, that is easily overpassed.

Nevertheless, people with OCD tend to have cognitive impairments including executive function (Snyder et al., 2015), attention (Koch et al., 2015), working memory (Harkin & Kessler, 2011) and non-verbal memory impairments (Savage et al., 1999). In clinics, after years of research, OCD heterogeneity is now characterized by using the Yale–Brown Obsessive Compulsive Scale (Y–BOCS) (Rosário-Campos et al., 2006). The basis of the scale relies on a ten-item questioner and in each item the patient scores the clinical severity of the disorder by rating the impact degree of the disorders in his life (from 0 to 4, being 0 - nothing and 40 - very severe). At the end of the test, clinicians are able to categorize each patient according to its obsessions type (*e.g.*: hoarding, washing, checking and fear of germ contamination) (Rosário-Campos et al., 2006). The causes for OCD are quite unknown, but there are multiple risk factors that can trigger or increase the probability of developing OCD, and those include: heritability (transmitted within families, due to genetic factors or a shared environment) (Nestadt et al., 2011); stress, as experiencing traumatic or stressful events (Adams et al., 2018); and other mental disorders (such as anxiety-like disorders, depression, substance abuse or tic disorders).

In summary, OCD is a multidimensional disorder that is included in the spectrum of anxiety disorders, as other obsessive-compulsive-related disorders, such as body dysmorphic disorders, trichotillomania and hoarding disorder, according to the *Diagnostic and Statistical Manual of Mental Disorders (DSM-5)* (APA, 2013).

### **1.2.2 Melanocortin 4 receptor as an indirect modulator of compulsive behaviors**

The MC4R is a subtype of the melanocortin receptor family that encodes for a membrane-bound receptor, which interacts with adrenocorticotrophic (ACTH) and melanocyte-stimulating (MSH) hormones. Firstly, MC4R was identified as a crucial molecule involved in the maintenance of body energy homeostasis (Adan et al., 2006; Pandit et al., 2015). Human studies have shown that MC4R mutations are a leading cause of autosomal dominant obesity (Farooqi & O'Rahilly, 2008). In that sense, after MC4R activation in

mice it was observed a decrease in food intake and an increase in energy expenditure (Balthasar et al., 2005). On the contrary, MC4R-null mice display a metabolic syndrome, similarly to the same phenotypic characteristics in humans, presenting insulin resistance and dyslipidemia (Bolze & Klingenspor, 2009).

MC4R is highly activated in the hypothalamus which is correlated with its involvement in food behavior but, recently, it was also observed an interaction with D1 MSNs in the ventral striatum (Cui et al., 2012; Lim et al., 2012). In accordance, stimulation of the MC4R-signaling in rats induced an unusual compulsive grooming behavior (Alvaro et al., 2003). Therefore, combining the role of MC4R in regulating feeding behaviors with the involvement of MC4R in the striatal circuits, Xu and colleagues (2013), studied the influence of MC4R in a well-established OCD-mice model: the synapse-associated protein 90/postsynaptic density protein 95-associated protein 3 (SAPAP3)-null mice (Xu et al., 2013). Interestingly, both constitutive and genetic deletion of *Mc4r*, as well as pharmacologic inhibition, ameliorated significantly the compulsive grooming and normalized striatal electrophysiological impairments in SAPAP3-null mice (Figure 3) (Xu et al., 2013).

Overall, new relevant insights of the pathophysiology of this neuropsychiatric disorder were revealed both in compulsivity and eating disorders, engaging a role for the MC4R. However, the mechanism through which this is occurring remains unknown. Nevertheless, the cause for MC4R-null mice obesity could be explained by LCN2 since it was shown that LCN2 binds to MC4R in the hypothalamus to regulate food intake; still, why the absence of the receptor leads to the behavioral normalization in the OCD-mice model remains unclear. Of importance, LCN2-null mice also display an anxious-like behavior, which is also a characteristic of OCD.

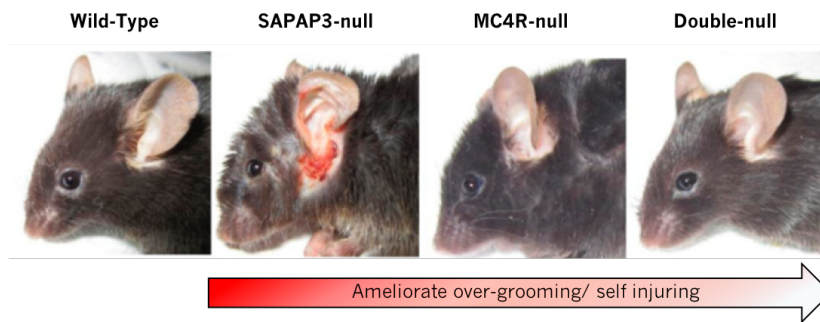


**Figure 3: Comparative compulsive outcome in different genetic mice.** Double genetic deletion of MC4R and SAPAP3 in mice restored normal behavioral features of facial lesions, a specific outcome of the SAPAP3-null mice, a well-established OCD-mice model (Adapted from (Xu et al., 2013)).

### 1.2.3 The role of the cortico-striato-thalamocortical circuitry

Finally, to link all the aforementioned information regarding OCD features, it is crucial to dissect the main pathway associated with the development of this neuropsychiatric disorder, the cortico-striato-thalamocortical circuitry (CSTC) (Pauls et al., 2014). Typically, CSTC is sub-organized in two circuits, the direct and indirect pathway, and the first (direct/excitatory) is modulated by the second (indirect/inhibitory) pathway (Figure 4) (Robertson et al., 2017). Fortunately, due to the high-technology available, patient neuroimaging screening has revealed important information of the disease's development. Overall, when OCD patients are compared to healthy individuals it is observed an hyperactivation of the CSTC due to an excessive activity of the cortical excitatory (direct) pathway over the cortical inhibitory one (indirect) (Figure 4) (Saxena et al., 2000). Briefly, OCD patients display an over-glutamatergic excitation of the striatum by the orbitofrontal cortex (OFC), that inhibits the GABAergic pathway to the globus pallidus interna (GPi) and substantia nigra (SNr). The outcome is observed in the obsessions experienced by the patients that are mediated by the OFC, that consequently lead to the compulsions (Figure 4).

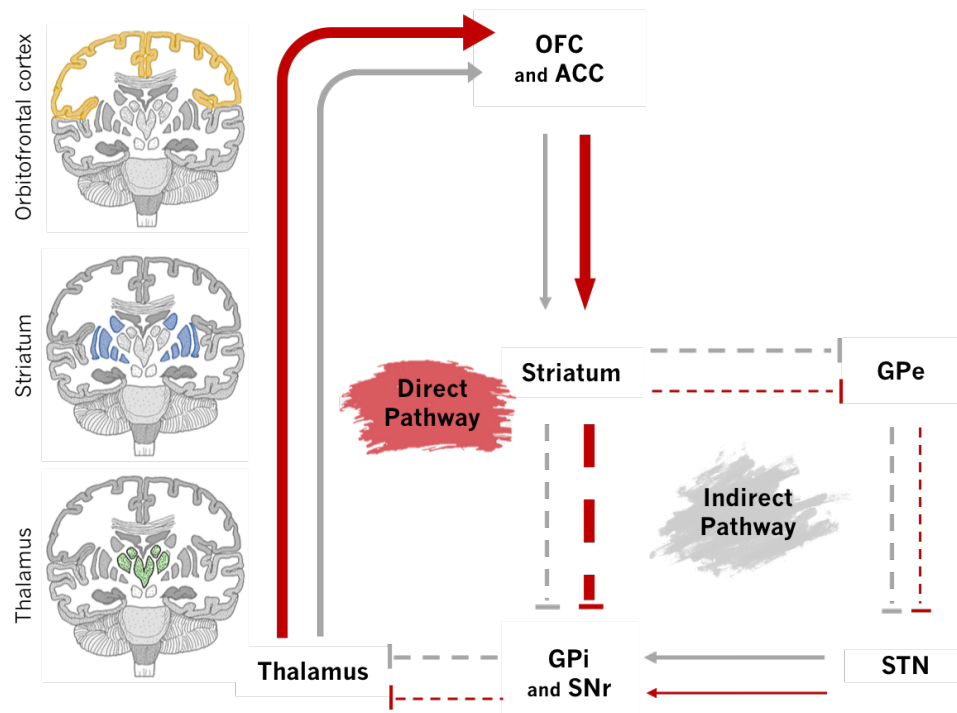


**Figure 4: The cortico-striato-thalamocortical circuitry comparing OCD patients to healthy individuals.** Solid arrows refer to glutamatergic excitatory pathways and dashed arrows the GABAergic inhibitory pathway. In the normal circuitry (grey arrows) mainly the orbitofrontal cortex (OFC) and the anterior cingulate cortex (ACC) lead glutamatergic signals, stimulating the striatum. Then, in the direct pathway, striatal activation leads to an inhibition of the globus pallidus internus (GPi) and the substantia nigra (SNr). Consequently, disinhibiting the thalamus outputs that excites the frontal cortex, resulting in a positive feedback loop. Alongside, in the indirect pathway, striatum inhibits the globus pallidus externus (GPe) which in turn disinhibits the subthalamic nucleus (STN). The STN is now available to excite the GPi and the SNr, finishing this external loop. In OCD patients (red arrows) there is an over activation of the striatum that promotes the direct pathway.

In summary, CSTC circuitry is the main altered pathway in OCD pathophysiology. Despite this knowledge, a deeper understanding regarding the functioning and molecular basis of the striatum is still necessary. Indeed, the striatum is a very complex region that receives the main inputs involved in the OCD loop. Therefore, striatum morphology, functioning and mediated-striatal-behaviors will be further discussed.

## 1.3 STRIATUM

### 1.3.1 An overview

The striatum is a common and convergent point, being the entry station of the basal ganglia. It is capable of interacting with cortical, thalamic and midbrain inputs (Kreitzer & Malenka, 2008). Of notice, the striatum is a crucial brain region associated mostly to motor functioning and learning procedures (Graybiel et al., 2015; Liljeholm et al., 2012), and it has been associated with multiple neurological disorders, such as Parkinson's (Porritt et al., 2000), Huntington's (Nopoulos, 2016) and OCD (Burguière et al., 2008). In Parkinson's disease, as it was previously mentioned, it is also observed an imbalance between the direct and indirect pathways of the CSTC by the loss of dopaminergic inputs to the striatum, resulting in impaired movement capabilities (Aosaki et al., 2010; Porritt et al., 2000). Further, in Huntington's a dysfunctional and degeneration of striatal projection neurons was described, leading to severe motor deficits (Nopoulos, 2016).

Briefly, the human striatum is subdivided by the internal capsule into caudate nucleus and putamen, where the first receives mainly excitatory inputs from the OFC, prefrontal (PFC), and cingulate cortex (Monteiro et al., 2016). On the other hand, putamen inputs are mostly received from the sensorimotor areas. As it is elucidated in Figure 5, the rodent brain does not exhibit a clear separation between caudate and putamen, however, it has a similar medial-lateral gradient of connectivity from the caudate (ventromedial) to the putamen (dorsolateral) (Monteiro et al., 2016). Additionally, in the dorsal striatum (DS), the ventral part receives mostly inputs from the associative cortical areas, while the lateral one from sensorimotor cortical areas.

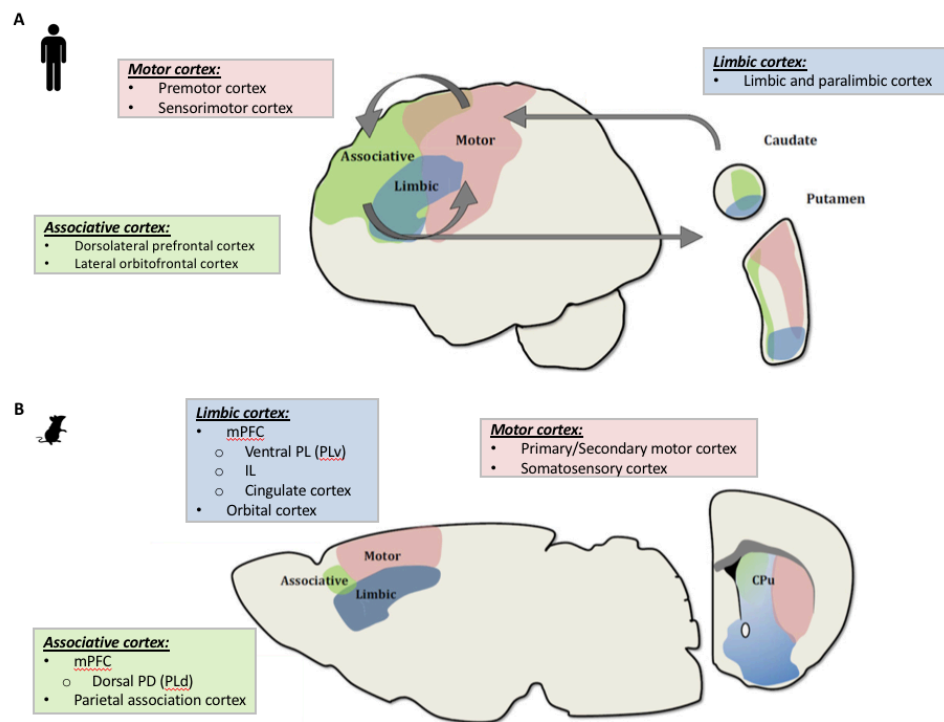


**Figure 5: Neuroanatomic differences between the cortico-striatal circuitry in humans (A) and mice (B) brains.** (Adapted from (Monteiro et al., 2016))

### 1.3.2 The role of striatum in Decision-Making

In their daily life, humans are prepared to make decisions. In fact, our actions are normally based on specific antecedents (stimulus) or performed depending on a certain consequence that we are expecting (outcome). Therefore, the way of how we react to some situations can be in a stimulus-reaction (habit action) way or in an action-objective way (goal-directed) (Dickinson, 1985; Hilario, 2008). To clarify, imagine that over the past ten years you and your mother lived in an apartment in the 3<sup>rd</sup> floor, and you are habitual to press the same button on the same elevator to reach your apartment. Now, you move to another apartment on the 5<sup>th</sup> floor. You reach the new elevator with your mother, and you press the button to the 5<sup>th</sup> floor (objective), but suddenly your mother presses the button to the 3<sup>rd</sup> floor (reaction). In this case, you are performing a goal-directed action, but your mother, on the contrary, is performing a habitual action that is controlled by an antecedent stimulus (the old apartment).

Although it still exists a big effort in the field to understand the anatomic and molecular basis behind these actions, the dorsal striatum is one of the neuroanatomical regions implicated in the control of decision-making (Figure 6) (Balleine et al., 2007). The

dorsomedial striatum (DMS) is responsible for the associative loop, in addition with the prelimbic (PL) subregion of medial prefrontal cortex (mPFC) and the mediodorsal thalamus (Atallah et al., 2007). The associative circuitry supports the learning of goal-directed actions (Voorn et al., 2004; Yin et al., 2005). On the other hand, the dorsolateral striatum (DLS) in association with the infralimbic (IL) cortex is involved in habit formation. Noteworthy, both corticostriatal circuits work in parallel and are intrinsically interconnected, which gives the possibility of switching between during action performance (Hilario et al., 2013; Voorn et al., 2004).

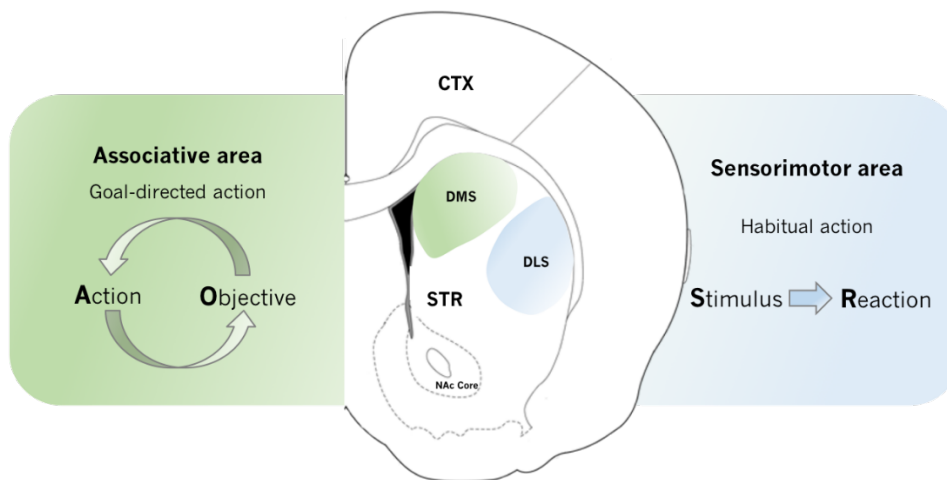


**Figure 6: Medial-lateral functional gradient of the dorsal striatum that is underlying goal-directed and habitual action strategies.** Representation of the dorsomedial striatum (DMS) (green) responsible for the associative circuitry that generates goal-directed actions. Dorsolateral striatum (DLS) (blue) mediates habit formation through stimulus-reaction responses. (The diagram illustrating a coronal section of the mouse brain was adapted from Paxinos and Franklin, 2001).

In the context of OCD, as discussed in the previous section, corticostriatal circuitry is described to be involved in the neurophysiology of the disease. Animal studies have linked the associative area (DLS) to aberrant grooming behavior in rodents, which is a common feature in OCD-mice models (Piantadosi & Ahmari, 2015; Welch et al., 2007). Repetitive behaviors are also observed in OCD patients that might result from a dysfunctional transition from DMS to DLS region (Ahmari et al., 2013; Gillan & Robbins, 2014). Besides their anatomical differences, the same behavioral transition is possible to be observed in mice by using operant conditioning (Hilario et al., 2008). Operant conditioning was first applied in rats by Dickinson *et al.*, to study the shift between goal-directed and habitual actions (Dickinson et al., 1985). Then in 2007, Hilario



and her colleagues applied operant conditioning to investigate the molecular mechanisms of habit formation, adapting Dickinson's work to mice (Hilario et al., 2007).

In summary, the striatum is a critical brain region involved in the regulation of several dimensions from motor to decision-making responses. Understanding the mechanisms that mediate such actions have been a main goal in the field and perceiving neuronal striatal cells diversity represents a useful tool to achieve it.

### 1.3.3 Neuronal striatal cells

Striatal neurons have been largely studied over the past few years to understand striatal functioning in health and disease. They can be classified in two main classes: (a) MSNs; and (b) interneurons (Kreitzer et al., 2009).

MSNs are spiny projection neurons that represent over 90% of the total striatal neurons. They are characterized by high spine density, low firing rates *in vivo*, markedly hyperpolarized resting potential, and inhibitory profile (GABAergic) (Tepper et al., 2004). Furthermore, MSNs can also be distinguished between them depending on their axonal projection and selective expression of neuropeptides and receptors. Striatonigral MSNs are involved in the direct-pathway, projecting to the substantia nigra pars reticulata (SNr) and globus pallidus internus (GPi). Selectively striatonigral MSNs are enriched in substance P and dynorphin and exhibit high expression of dopamine (DA) D1 receptor (D1R) and M4 muscarinic acetylcholine (ACh) receptor (Bertran-Gonzalez et al., 2010). On the other hand, in the indirect striatopallidal pathway, MSNs project mainly to the GP. Striatopallidal MSNs contain enkephalin and express D2 (D2R) and A2a adenosine (A2aR) receptors (Bertran-Gonzalez et al., 2010; Kreitzer & Malenka, 2008).

Striatal GABAergic interneurons are aspiny cells that can be categorized based on their physiological differences: (a) fast-spiking; and (b) low-threshold spiking; and/or also in their histochemical differences: (a) parvalbumin-positive cells; (b) somatostatin-, nitric-oxide-synthase-, and neuropeptide-Y-positive cells; and (c) calretinin-positive interneurons (Kreitzer, 2009). Fast-spiking cells, as the name indicates, exhibit a rapid and sustained firing rate and correspond to the parvalbumin-positive cells. Further, low-threshold spiking cells include somatostatin-, nitric-oxide-synthase-, and neuropeptide-

Y-positive cells and, possibly, calretinin-positive interneurons, that present a low firing rate and plateau potentials (Kreitzer & Malenka, 2008). Finally, the remaining cells are the aspiny cholinergic interneurons (ChIs). Anatomically, ChIs are the larger interneurons when compared to the previous ones and, are considered as the main source of striatal Ach. Besides, ChIs are characterized by their spontaneous activity and hyperpolarization-activated currents under physiological conditions (Lim et al., 2014).

## CHAPTER 2

---

### 2. AIMS



OCD is a very debilitating clinical disorder that compromises the lives of patients and their families. Many efforts have been made in this field in order to find novel solutions to ameliorate disease-associated symptoms. MC4R has been implicated as an important mediator of compulsive behaviors; however, the mechanisms behind it are still unclear. Noteworthy, it was recently shown that LCN2 is a novel MC4R ligand and that, by binding to this receptor in the hypothalamus, it can suppress food intake, which is considered one type of compulsive behavior (Figure 7). Thus, in this thesis we hypothesized a role for LCN2 signaling, through the MC4R, in mediating compulsive behaviors in the striatum. To achieve this greater objective, we started by defining an initial task to characterize striatal-dependent behaviors in LCN2-null mice, and to better understand the impact of LCN2 in the regulation of striatal function. Therefore, our aims were to:

1. Explore the involvement of LCN2 in striatal-dependent behaviors;
2. Perform morphological and functional characterization of LCN2-null mice in the striatum;
3. Evaluate the expression of genes, in LCN2-null mice, that might be regulating striatal alterations.

Collectively, with this thesis, we aim to contribute to the knowledge on how LCN2 modulates the striatum, and how this modulation can be translated at the behavioral level that might be related to the OCD phenotype.



## CHAPTER 3

---

### 3. MATERIAL AND METHODS





### 3.1 Experimental Animals

In this thesis, mouse strain with a specific targeted deletion of the *Lcn2* gene (LCN2-null mice), and their respective wild-type (WT) littermate controls, was used. LCN2-null mice strain was achieved by a disruption of an entire coding sequence (exons 2 to 5), which was replaced with a neomycin (Neo) cassette, resulting in the deletion of the target gene, as it is shown in Figure 8.

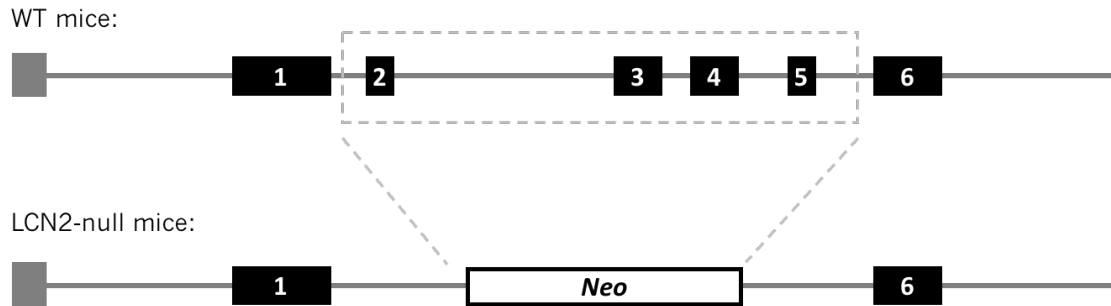


**Figure 8: LCN2-null mice model.** Replacement of an entire coding sequence, from the exon 2 to 5 (black boxes) with a neomycin (Neo) cassette (white box).

All experimental procedures were conducted and approved by the Portuguese National Authority for animal experimentation, *Direção Geral de Veterinária* (ID: DGV9457). Animal housing and handling was in accordance with the guidelines for the care and wellbeing of laboratory animals in accordance with the Directive 86/609/EEC of the European Parliament and of the Council. All mice were bred and maintained at the Life and Health Sciences Research Institute animal facilities and, to improve and ensure the animals welfare, efforts were made to minimize the number of animals used and their suffering. All mice were fed with standard diet (4RF25 during gestation and postnatal periods, and 4RF21 after weaning; Mucedola SRL, Settimo Milanese, Italy) and water was provided *ad libitum*. Husbandry conditions were maintained in accordance with standard conditions, on a 12/12-h light/dark cycle (lights on at 8 a.m.) with an ambient temperature of  $21\pm 1^{\circ}\text{C}$  and relative humidity of 50-60%. In order to maintain the colony and the prevalence of this particular genotype, matings were strictly performed as it is shown in Figure 9.

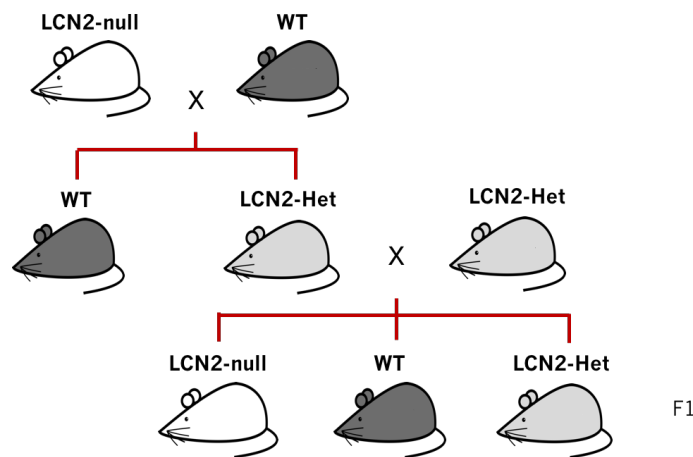


**Figure 9: Colony management strategy to maintain LCN2-null mice and WT littermate controls phenotype.** LCN2-null mice were bred with WT mice to obtain LCN2-Het mice. In return, LCN2-Het mice were bred for different generations in order to have LCN2-null mice and the respective WT littermate controls.

First, WT and LCN2-null (kindly given by Professor Trude Flo) mice were bred to obtain LCN2-Het mice. From then on LCN2-Het mice were mated amongst them (LCN2-Het x LCN2-Het), to obtain WT and LCN2-null mixed litters to perform the experimental procedures for this thesis. The breeding programme was as follows: whenever a mouse was born it was kept untouched in its home cage with their mothers until weaning was performed at 21 days of age; then, males and females were separated and kept in different cages, in groups of five to seven animals per cage (530 cm<sup>2</sup>), depending on their weight, until genotyping; for genotype determination, animals were identified in the ear or tail. Our animals were raised in a C57BL/6 background.

### 3.2 Genotyping

Genotypes of LCN2-null, Het and WT mice were determined by a polymerase chain reaction (PCR). As a first step, after collecting a representative biological sample (ear or tail tip), DNA was extracted by digestion. To each tube, it was aliquoted 300 µl of NaOH (50mM) solution following by a digestion step at 98°C, for 50 minutes (min). Then, samples were vortex for 15 seconds (sec) and neutralized with 30 µl of 1M Tris (pH=8.0). After a centrifugation step of 14 000 rpm for 6 min the supernatant was removed. The PCR strategy relied on the amplification of the junction of the Neo cassette with the target gene flanking sequences, as it is explicit in Figure 10.

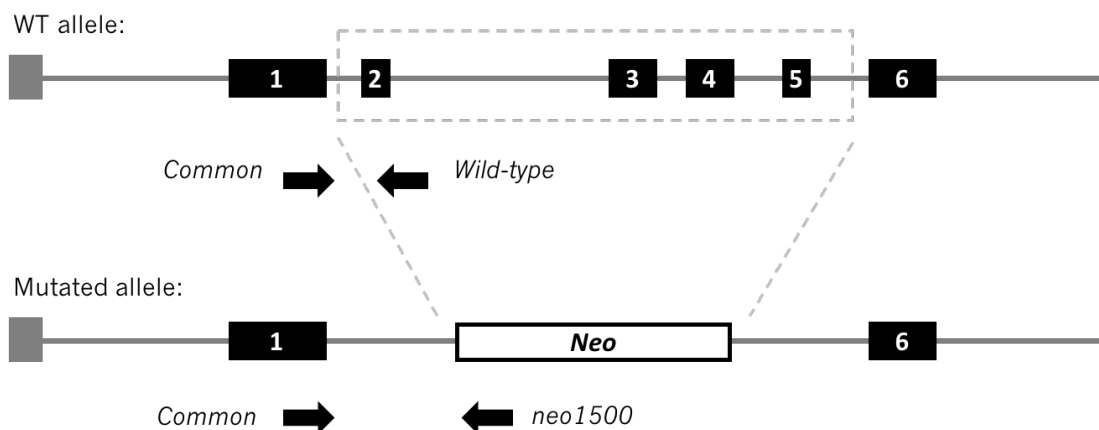


**Figure 10: Schematic representation of the genotype strategy used to identify LCN2-null mice.** The exons are represented in black boxes and the Neomycin (Neo) cassette in white box. Both alleles have 500 bp therefore, WT allele amplification is accessed with *Common* and *Wild-type* primers, while *neo1500* and *Common* primers are used to identify the mutated allele.

For the detection of both mutated and WT alleles, it was necessary to design three independent primers, *Common*, *Neo1500* and *Wild-type* (Table 1).

**Table 1: Primer sequences for the polymerase chain reaction (PCR).**

Primer Denomination	Primer sequence (5' → 3')	TM (°C)
<i>Common</i>	ATCCGGTTCTATCGCCTTCTTGACGAG	
<i>Neo1500</i>	GTCCTTCTCACTTTGACAGAAGTCAGG	58
<i>Wild-type</i>	CACATCTCATGCTGCTCAGATAGCCAC	

The *Common* primer is specific for *Lcn2* gene and, in combination with either *neo1500* or *Wild-type* primers allows to distinguish between LCN2-null mice and WT, respectively. Therefore, Het mice have both bands, however, since the product size in both sets of primers is 500 bp, it is required to perform two independent PCR reactions. For each PCR reaction, was used 1 µl of DNA (100 ng/µl) for a final volume of 20 µl, using the mix and reaction conditions described in Table 2.

**Table 2: PCR Mix components and PCR conditions for genotyping strategy.**

Master Mix (vt=20µl)	Volume (µl)	DNA template	PCR reaction conditions	
<b>H<sub>2</sub>O</b> <sup>1</sup>	14.5		<b>Temp</b>	<b>Δt</b>
<b>MgCl<sub>2</sub></b> (25 mM) <sup>2</sup>	1.2		(°C)	
<b>dNTPs</b> (10 mM)	0.4		95	2'
<b>Taq Buffer</b> (with (NH <sub>4</sub> ) <sub>2</sub> SO <sub>2</sub> ) <sup>2</sup>	2.0		95	1'
<b>Taq Polymerase</b> (5 U/µl) <sup>2</sup>	0.1	<b>1 µl</b>	58	45''
<b>Common</b> (20 µM)	0.4		72	1'
<b>Neo1500</b> (20 µM)	0.4		72	5'
<b>Wild-type</b> (20 µM)	0.4		4	∞

<sup>1</sup>Sigma Aldrich, St. Louis, Missouri, USA  
<sup>2</sup>Fermentas Life Science, California, USA

The amplified PCR products were separated in a 1.5% agarose gel, stained with Safe-green<sup>TM</sup> and revealed under UV illumination.

### 3.3 Behavioral procedures

For behavioral assessments, adult male LCN2-null and WT littermate mice of 2-3 months of age were used. To ensure animals' well-being, behavioral tests were not performed consecutively but with a minimum of one day of interval between tests.

#### 3.3.1 Operant conditioning test

To analyze for LCN2 effects on decision-making an instrumental/operant conditioning test was performed. More in detail, the current test aimed to analyze goal-directed behavior responses in mice, which are highly dependent on the DS. During the behavioral training and testing, two independent groups of animals were used ( $n_{WT} = 8$ ,  $n_{LCN2-null} = 8$  per group in each experiment). For this behavioral test, operant chambers (30.5 cm L × 24.1 cm W × 21.0 cm H) housed within sound attenuating chambers (Med Associates, Inc. St. Albans, VT, USA) were used. Each chamber was equipped with two retractable levers on either side of the food magazine. The chamber had also a pellet dispenser to deliver food and a house-light (3W, 24V) placed on the other side of the chamber. Chambers were controlled by Med-PC on the desktop computer (Med Associates, Inc., St Albans, USA). Approximately 1 week before beginning the training, mice were properly handled, weighted and individually marked. Three days before starting the

training, all animals were submitted to a food deprivation schedule: on the first day animals only received 2 g of food; on the following day 1 g; and on the last day they were deprived from food. Gradual food deprivation was closely monitored to ensure that mice maintain their body weight above 85% of the baseline weight. At the same time, mice were acclimatized to chambers before starting the training during these three days. Throughout the following experimental days, mice were daily feed after the sessions with home-cage chow receiving an adjusted amount of food sufficient to maintain mouse's weight at 85% of free-feeding weight. The water was given *ad libitum* during the training days.

The training schedule was divided in two different stages: a fixed ratio stage and a random ratio stage. The main goal of training sessions was to allow animals to learn how lever pressing is associated with food pellets reward. The first stage, the fixed ratio 1 (FR-1) schedule is based on the delivery of one pellet per each lever press. Every time the session begins, the house light turned on and one lever was inserted into the chamber. The FR-1 session had a maximum period of 60 min or when the animal earned a total of 50 pellets. At the end of each session, the light house is turned off and the lever retracted. For three days, mice were submitted to FR-1 schedule to acquire consistent lever pressing. Although all animals learned to press the lever during these three days, to reach behavioral criteria animals should complete the task before 60 min, or closely reach 50 pellets ( $\geq 47$  pellets). Once completed, the animals initiated the second stage by beginning the random ratio training. First, a random ratio 10 (RR-10) was used for two days, where on average 1 pellet is delivered every 10 lever presses. Then the training was switched to a random ratio 20 (RR-20; on average after 20 lever presses animals earn 1 pellet) for four days (Figure 11). During these stages, data analysis was performed based on the number of presses per min and the number of rewards delivered per minute.

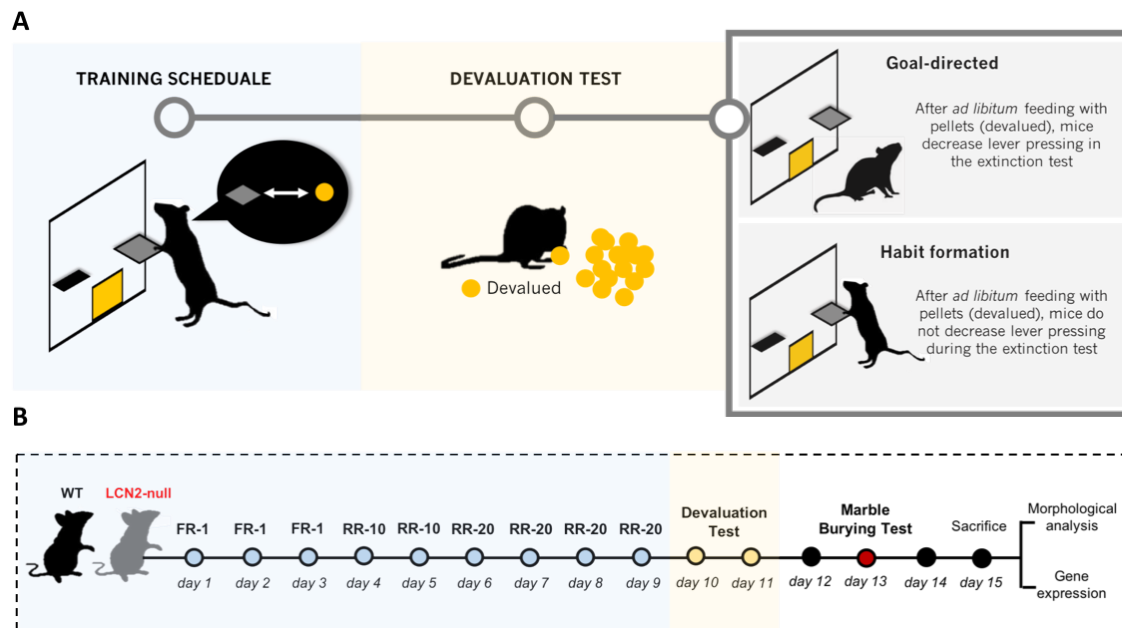


**Figure 11: Schematic representation of the operant task.** (A) Mice were first trained for a reinforcement in an operant box, where they have to lever press to get it. Then, devaluation test was performed for two days. The assessment is performed through a 5 min extinction test in operant chamber with the respective lever. At the end, the number of lever presses are compared between days and groups. If the presses under the valued condition are higher when compared to the devalued conditions then, the mouse had adapted a goal-directed behavior. Otherwise, if the lever press rate is equal the mouse is classified with a habitual lever pressing behavior. (B) Timeline schedule representation.

Once finished the training phase, mice were tested in a devaluation test in two different days (Dickinson et al., 1985) (Figure 11). At the beginning of each test day, mice were alternately exposed to one type of food (home-cage chow or pellets; in a total of 3.5 g per mouse) and water in individual and clean cages (free of bedding). For 1-hour mice were left under these conditions undisturbed to access all the food they want. All these details of mice consuming either the pellets earned by lever pressing (devalued condition), or the cage home chow (valued condition) in different days, was to ensure that devaluation test was achieved by a food sensory-specific satiety (Dickinson et al., 1985; Hilarion et al., 2007). During the one-hour *ad libitum* feeding, the amount of food consumed was recorded, and mice that did not consume a minimum of 0.4 g were given more time to eat. After the *ad libitum* feeding, mice were placed in the respective chamber for a 5 min test in extinction with the training lever extended. To evaluate valued and devalued conditions, animals were counterbalanced and the number of lever presses at the extinction test for each condition was recorded. Finally, devaluation index was calculated

based on the lever presses performed in extinction for 5 minutes. These results were also normalized to the number of lever presses done on the last day of RR-20 training.

### 3.3.2 Marble burying test

To assess repetitive and anxious-like behavior, marble burying test was performed (Deacon, 2006) two days after the previously described test in order to allow animals restoring their weight. At the test day, all animals were transported to the test room 60 min before to room acclimatization. Previously to test performance, standard mice cages (370 cm<sup>2</sup>) were carefully prepared with filter-top covers. Cages were approximately filled with 5 cm depth of mouse bedding material, that was carefully tamped down to make a flat surface. Clean standard glass marbles (assorted styles and colors, 15 mm diameter,  $\pm$  5.2 g in weight) were placed on the cage surface in a regular pattern spaced each 4 cm apart. Before place the animals, a picture was taken to the cage (*before*). Animals were placed in each cage very carefully and as far from marbles as possible. They were left for a total of 30 min undisturbed in the room. After completing the test, animals were carefully removed and returned to their home cages. By the end, a new picture was taken (*after*). The evaluation was performed by two different observers that counted the number of marbles buried, in a blind manner regarding animals' genotype. To assess it, scores were given considering the marbles that were more than two-thirds buried of its surface area. At the end, all the scores were averaged for the number of marbles buried for each mouse. As a last instant, pictures were compared (*before* and *after*) to confirm the analysis, where a higher digging rate is related with a higher repetitive and anxious-like behavioral phenotype.

### 3.4 Golgi-Cox staining

Adult mice brains of 2 and 3-months old ( $n_{WT} = 7$ ,  $n_{LCN2-null} = 7$ ) were transcardially perfused with 0.9% saline under deep pentobarbital anesthesia (Imalgene and Dorbene anesthetics in 0.9% saline solution for a total volume of 19.5 ml) and processed for Golgi-Cox staining according to the protocol described elsewhere (Gibb & Kolb, 1998). Briefly, during sacrifice, all the brains were carefully removed and immersed in Golgi-Cox solution (a 1:1 solution of 5% potassium dichromate and 5% mercuric chloride diluted 4:10 with 5% potassium chromate) (Glaser & Van der Loos, 1981) for 14 days. Then, brains were transferred to an 30% sucrose solution (minimum 5 days), before being cut

on the vibratome. Coronal sections (200  $\mu\text{m}$ ) were collected into 6% sucrose and mounted in gelatin-coated microscope slides. Subsequently, they were alkalinized in 18.7% ammonia, developed in Dektol (Kodak, Linda-a-Velha, Portugal), fixed, dehydrated through an ethanol graded series, cleared in xylene and mounted with entellan® (Merck Millipre, Portugal). To minimize bias, brain slides were coded before morphometric studies to perform a blind analysis.

### 3.5 Structural dendritic tree analysis

Three-dimensional (3D) reconstructions of representative Golgi-impregnated neurons at the DS were performed. Both dorsomedial striatum (DMS) and dorsolateral striatum (DLS) were analyzed since they represent distinct physiological, behavioral and connectivity roles. The reconstructed neurons were selected according to the criteria described by Uylings (1986) and Radley (2004):

- i) full impregnation of the neurons along the entire length of the dendritic tree;
- ii) dendrites without truncated branches;
- iii) relative isolation from neighboring impregnated neurons to avoid interference with the analysis;
- iv) no morphological changes attributable to incomplete dendritic impregnation of Golgi-Cox staining (Radley et al., 2004; Uylings et al., 1986).

To perform a more reliable analysis and minimize bias selection, in each brain the first neurons fulfilling the criteria (maximum of 3 neurons per slice) were randomly selected in the region of interesting. For each selected neuron, all dendritic tree branches were reconstructed at 600x magnification using a motorized microscope (BX51, Olympus, Hamburg, Germany), with oil objectives, attached to a camera (MicroBrightField Bioscience, Magdeburg, Germany) and with NeuroLucida software (MicroBrightField Bioscience). Three-dimensional analysis of the selected reconstructed neurons was achieved using NeuroExplorer software (MicroBrightField Bioscience). In both genotype groups, it was studied a total of ten neurons per region per animal, in a blind manner, and the average was assessed at the end for each animal. Dendritic morphology was then



explored, examining several aspects. Overall alterations, such as total dendritic length, the percentage of spines on dendrites and spine density (total number of spines divided by the dendritic length) were assessed by comparing the LCN2-null mice with the littermate WT group. Since the neurons present in the striatum are MSNs, which are radial neurons, dendritic spine density was determined by following the respective criteria:

- i) dendritic branches were either parallel or at acute angles to the coronal surface of the section;
- ii) did not show overlap with other branches that would obscure visualization of spines;
- iii) were at a radial distance of the soma between 40 to 60  $\mu\text{m}$ .

To assess spine morphology, all the spines in the selected dendritic segments were classified in: filopodia, thin, thick, stubby, mushroom and branched. Such classification was performed according to some specific morphological characteristics as it is demonstrated in

Figure 12. At the end, the proportion of spines in each category was compared between both groups.

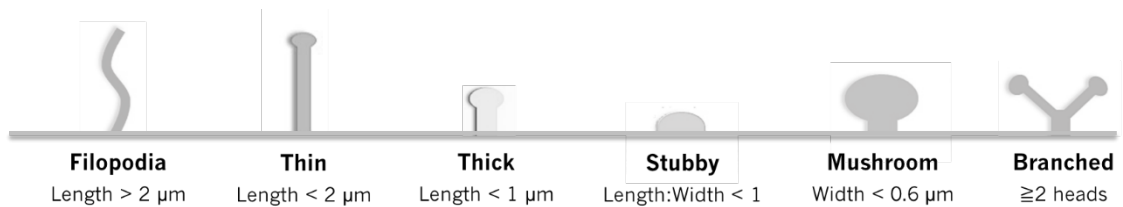


**Figure 12: Spine morphology classification.** Schematic drawing of the different spine classified according to their structural organization, which are mostly based on their length and width.

Finally, a 3D version of a Sholl analysis (Sholl, 1956) was performed to explore differences in the dendritic arrangement in both groups. Briefly, this analysis corresponds to the registration of the total number of intersections of dendrites with concentric spheres positioned at radial intervals of 20  $\mu\text{m}$  from the soma. All measurements for individual neurons from each animal were averaged.

### 3.6 Gene expression analysis

#### 3.6.1 RNA extraction and quantification

Total RNA from macro dissected striatal region was isolated ( $n_{WT}=11$ ,  $n_{LCN2-null}=11$ ) using TRIzol® Reagent method (Invitrogen, Carlsbad, CA, USA). Briefly, 1 mL of TRIzol® was added to the frozen tissue samples, which were mechanically disrupted using a 20 G needle. Then, samples were incubated at room temperature (RT) for 2-5 min and 200  $\mu$ L of chloroform (Sigma Aldrich, St. Louis, Missouri, USA) was added to each one and thoroughly mixed. Following, samples were incubated for 2-3 min at RT and centrifuged for 15 min at 8000 rpm and 4°C. The upper aqueous phase, the one that contains RNA, of the centrifuged samples was removed and recovered to new Eppendorf tubes, and mixed with 500  $\mu$ L of isopropanol (Sigma Aldrich, St. Louis, Missouri, USA) to precipitate RNA. After agitation, samples were incubated for 10 min at RT and centrifuged for 10 min at 9000 rpm, 4°C. The supernatant was removed, and the RNA pellet was washed with 50  $\mu$ L of 75% ethanol and centrifuged for 7 min at 6000 rpm, 4°C. After, ethanol was completely removed from the samples, dried isolated RNA pellet was resuspended in 20  $\mu$ L of RNase/DNase-free water (Sigma Aldrich, St. Louis, Missouri, USA). RNA concentration was determined by using NanoDrop® (Thermo Fisher Scientific, USA) and purity was inferred using the absorbance ratio at  $A_{260}/A_{280}$  and  $A_{260}/A_{230}$ .

#### 3.6.2 DNase/RNase-free treatment

After RNA isolation, in order to remove the maximum of genomic DNA that might be present in samples, 2  $\mu$ g of RNA were placed in a new RNase free tube with 1 U of DNase I (Thermo Fisher Scientific, USA) per microgram of RNA, 10xBuffer with  $MgCl_2$  and RNase/DNase-free water (Sigma Aldrich, St. Louis, Missouri, USA) to a total volume of 10  $\mu$ L. Then samples were incubated at 37°C for 30 min and 1  $\mu$ L of 50 mM EDTA was added and samples were incubated for 10 min at 65°C. Finally, they were placed into ice and again quantified using the NanoDrop® system.

### 3.6.3 Complementary DNA (cDNA) synthesis

Reverse transcription of RNA was performed using the iScript™ Advanced cDNA Synthesis Kit (Bio-Rad, Hercules, CA, USA) according to the manufacturer's instructions. Briefly, the reaction mix comprised 4 µL of 5x iScript reaction mix, 1 µL of iScript reverse transcriptase, 500 ng of treated RNA and nuclease-free water for a final volume of 20 µL. The cDNA synthesis reaction was performed in a thermocycler (Eppendorf, Hamburg, Germany), for 5 min at 25°C, 30 min at 42°C followed by a final step of 5 minutes at 85°C. The resultant cDNA template was further stored at -20°C until further use.

### 3.6.4 Quantitative Real-Time PCR (qRT-PCR) gene expression analysis

For the qRT-PCR, 1 µL of each cDNA samples was carefully mixed with 3 µL of RNase free water, 0.5 µL of 10 µM forward and reverse specific primers, and 5 µL of SoFast™ EvaGreen® Supermix (Bio-Rad, Hercules, CA, USA). The qRT-PCR was performed in CFX96™ Real-time system (Bio-Rad, Hercules, CA, USA) using the following program: an initial denaturing cycle at 95°C for 1 min, followed by 40 amplification cycles of 95°C for 15 seconds, 20 seconds at the specific temperature of annealing ( $T_a$ ) for each primer, and 72°C for 20 seconds. Finally, an additional step ranging from 65°C to 95°C, with a progressive increment of 0.5°C for 5 sec, was included to determine the melting curves. Relative mRNA expression for the specific target genes was normalized to the levels of housekeeping genes using the  $\Delta C_t$  method as follows:  $1.8^{(Housekeeping\ gene\ mRNA\ expression - Target\ gene\ mRNA\ expression)} \times 100000$ , and all the data was analyzed by using the programme "Bio-Rad CFX Manager". For relative analysis of gene expression two different sets of housekeeping primer genes were used (*Hspcb* and *Atp5b*). Primer sequences used for the relative quantification analysis are listed in Table 3.

**Table 3: Primers sequences used to determine the relative expression of a target gene using the qRT-PCR method.** The annealing temperature (°C) as efficiency rate were determined for each set of primers.

Target gene	Forward Primer sequence (5' → 3')	Reverse Primer sequence (5' → 3')	Ta (°C)
<i>Syp</i>	CTGCGTTAAAGGGGGCACTA	GGAAGTCCATCATTGGCCCT	60
<i>D1 receptor</i>	TCTCCAGATCGGGCATT	GTCCCTAGATTCCCCAAGGA	61
<i>D2 receptor</i>	ATCGTCTCGTTCTACGTGCC	GTGGGTACAGTTGCCCTTGA	60
<i>Ampa</i>	TGGTGGTACGATAAAGGGGA	AGCCCTCCAATCAGGATGTA	60
<i>Gaba</i>	TTTGGGAGAGCGTGTAAGT	TAAGGTTGTTTAGCCGGAGC	60
<i>Nmda</i>	GCATCCACCTGAGCTTCCTT	TTCTCTGCCTTGGACTCACG	60
<i>Psd-95</i>	ATTGCGGAGGTCAACACCAT	TTCTCAGCACCTGGACAATGA	60
<i>Mc4r</i>	ATCTGTAGCTCCTTGCTCGC	TGCAAGCTGCCAGATACAA	61
<i>Sapap3</i>	CACCATGTAACCCCGGCTG	GCCCCAGGAACCTCCATC	60
<i>Shank3</i>	AGGAACTTGCTTCCATTCGGA	ATCTCAGCAGGGGTGATCCT	60
<i>Hspcb</i>	GCTGGCTGAGGACAAGGAGA	CGTCGGTTAGTGGAATCTTCATG	60
<i>Atp5b</i>	GGCCAAGATGTCCTGCTGTT	GCTGGTAGCCTACAGCAGAAGG	60

### 3.7 Slice electrophysiology

Acute striatal slices from two independent experiments (n<sub>WT</sub>=3, n<sub>LCN2-null</sub>=3 mice per each experiment) were prepared for the electrophysiological recordings. Briefly, animals were deeply anaesthetized with avertin (tribromoethanol; 20 mg/mL) (Sigma Aldrich, St. Louis, Missouri, USA) at a dose of 0.5 mg/g body weight by intraperitoneal injection. Then animals were transcardially perfused with 15–20 ml oxygenated NMDG (N-methyl-D-glucamine) solution (Table 4) (Sigma Aldrich, St. Louis, Missouri, USA). After decapitation, brains were rapidly removed and placed in the same solution for slice preparation. A vibratome VT1200S (Leica Microsystems, Wetzlar, Germany) was used to prepare the 300 µm thick striatum coronal slices. Slices were incubated at 32°C for 11 min in oxygenated NMDG solution and then transferred to holding chamber containing artificial cerebrospinal fluid (aCSF) solution (Table 4) (Sigma Aldrich, St. Louis,

Missouri, USA) at RT for at least 1 hour to allow the slices to recover. Recordings were made at RT with chloride silver electrodes. Patch pipettes were pulled from borosilicate-glass on a Flaming-Brown puller with a typical resistance of 2-5 M $\Omega$  when filled with cesium gluconate internal solution (Table 4) (Sigma Aldrich, St. Louis, Missouri, USA). MSNs at the DMS were identified under infrared differential interference contrast (IR-DIC) using a BX-51WI microscope (Olympus). Drug application of Picrotoxin (PTX, 100  $\mu$ M), an antagonist of GABA<sub>A</sub> receptor, and Tetrodotoxin (TTX, 1  $\mu$ M), a sodium receptor blocker, (all from Tocris Bioscience, Bristol, UK) was done through a gravity fed system. The signals for voltage clamp were filtered at 2 kHz and digitalized at 10 kHz with a Digidata 1440A and a MultiClamp 700B amplifier. All data was analyzed using the Mini Analysis Program V6.0.7 (Synaptosoft, Inc., Decatur, GA, USA). This task was performed in collaboration with Diana Rodrigues and Patrícia Monteiro.

**Table 4: Solution reagents list used during the slice electrophysiological protocol.**

	Chemical reagent	Abbreviation	mM	pH	Osmolarity	Supplier
Oxygenated NMDG solution	N-methyl-D-glucamine	NMDG	92.00			
	Potassium chloride	KCl	25.00			
	Sodium dihydrogen phosphate	NaH <sub>2</sub> PO <sub>4</sub>	1.20			
	Sodium Bicarbonate	NaHCO <sub>3</sub>	30.00			
	4-(2-hydroxyethyl)-1-piperazineethanesulfonic acid	HEPES	20.00			
	Glucose	C <sub>6</sub> H <sub>12</sub> O <sub>6</sub>	25.00			
	Sodium ascorbate	C <sub>6</sub> H <sub>7</sub> O <sub>6</sub> Na	5.00			
	Thiourea	CH <sub>4</sub> N <sub>2</sub> S	2.00			
	Sodium pyruvate	C <sub>3</sub> H <sub>3</sub> NaO <sub>3</sub>	3.00			
	Magnesium sulfate heptahydrate	MgSO <sub>4</sub> ·7H <sub>2</sub> O	10.00			
	Calcium chloride	CaCl <sub>2</sub> ·2H <sub>2</sub> O	0.50			
aCSF solution	Sodium chloride	NaCl	119.00			
	Potassium chloride	KCl	2.50			
	Sodium phosphate monobasic	NaH <sub>2</sub> PO <sub>4</sub>	1.20	7.2	300	Sigma-Aldrich (Missouri, USA)
	Sodium Bicarbonate	NaHCO <sub>3</sub>	24.00	-	±	
	Glucose	C <sub>6</sub> H <sub>12</sub> O <sub>6</sub>	12.50	7.4	10	
	Magnesium sulfate heptahydrate	MgSO <sub>4</sub> ·7H <sub>2</sub> O	2.00			
Calcium chloride dehydrate	CaCl <sub>2</sub> ·2H <sub>2</sub> O	2.00				
Cesium gluconate internal solution	Cesium hydroxide	CsOH	110.00			
	D-Gluconic acid	C <sub>6</sub> H <sub>12</sub> O <sub>7</sub>	110.00			
	Potassium chloride	KCl	15.00			
	Sodium chloride	NaCl	4.00			
	Tetraethylammonium Chloride	TEA-Cl	5.00			
	4-(2-hydroxyethyl)-1-piperazineethanesulfonic acid	HEPES	20.00			
	Ethylene glycol-bis(2-aminoethylether) -N,N,N',N'-tetraacetic acid	EGTA	0.20			
	Lidocaine N-ethyl chloride	C <sub>16</sub> H <sub>27</sub> N <sub>2</sub> OCl	5.00			
	ATP·xMg <sup>2+</sup>	-	4.00			
	GTP·xNa <sup>+</sup>	-	0.30			

### 3.8 Statistical analysis

Statistical analysis was performed using the GraphPad Prism 5 (GraphPad software Inc., La Jolla, CA, USA). Data are represented as mean  $\pm$  standard error of the mean (SEM) for parametric tests and, when non-parametric tests were applied data are represented as median  $\pm$  interquartile range (IQR). Sample normality distribution was assessed with Shapiro-Wilk test. To compare both genotypes, the parametric Student's t-test was used for samples with normal distribution. The non-parametric Mann-Whitney and Wilcoxon Rank Sum and Signed Rank tests were used for samples without normal distribution. For Sholl analysis and training curves during the operant conditioning task a two-way repeated measures ANOVA, with Bonferroni multiple comparison post-hoc test, was used. In the analysis for the cumulative probability in electrophysiological records, the non-parametric Kolmogorov-Smirnov test was applied. The Cohen's d and eta-squared value ( $\eta^2$ ) were calculated as a measure of effect size for t-tests and two-way repeated measures ANOVA, respectively (Tomczak et al., 2014). Values were considered significant for  $p \leq 0.05$  and represented with \* for  $p \leq 0.05$ ; \*\* for  $p \leq 0.01$ , \*\*\* for  $p \leq 0.001$ , and \*\*\*\* for  $p \leq 0.0001$ .





CHAPTER 4

---

**4. RESULTS**



Based on evidences that: i) LCN2 is able to bind MC4R in the hypothalamus, which results in altered food intake behaviors, a type of compulsive behavior and, ii) that by an unknown mechanism, the deletion of *Mc4r* is able to rescue compulsive behaviors in an animal model of human OCD; we hypothesize that this can be mediated by its ligand LCN2 (Figure 7). Herein, we aimed at unravelling if LCN2 is somehow regulating compulsive behaviors in the striatum, and if this regulation is through MC4R. For that, we performed a battery of experiments in LCN2-null mice and their respective littermate controls to assess: i) behaviors striatal-dependent, ii) neuronal electrophysiological functional properties and neuronal morphology at the striatum, and iii) a general molecular characterization of genes related to striatal synapses

#### 4.1 Decision-making is biased in the absence of LCN2

Based on our aim, we started by characterize striatal-dependent behavior in LCN2-null mice when compared to WT. In this task, we intend to analyzed whether the absence of LCN2 is affecting the ability of mice to perform an instrumental test that is based on striatal function (C. D. Adams & Dickinson, 1981).

As it is illustrated in Figure 13A, both groups increased lever pressing across training schedule and no main effect or interaction was observed between groups (Table 5), meaning that WT and LCN2-null mice learned equally. In the same sense, the rate of reinforcers per min was also calculated, and no significant difference were found (Figure 13B, Table 5), ensuring that both groups learned similarly.

At the end of the training and lever pressing acquisition, devaluation test was performed based on the expected value of the outcome delivery (Figure 13C) to test for decision-making. During the two days of devaluation test, (*see Material and Methods* – Figure 12) mice were assessed for a 5 min extinction test in the chambers to record the number of lever presses.

**Table 5: Statistical analysis performed during the instrumental task, both during training and devaluation test in LCN2-null mice and littermate controls.** Data presented as mean  $\pm$  SEM for parametric tests, and as median  $\pm$  IQR for non-parametric tests. Statistical differences are reported as \*\* for  $p \leq 0.01$ .

<i>TRAINING</i>		Statistical test, significance, effect size	
<b>Lever presses per min</b>			
• Genotype factor		$F_{1,15}=0.287; p=0.600$	
• Interaction		$F_{8,120}=0.459; p=0.882$	
<b>Reinforcements per min</b>			
• Genotype factor		$F_{1,15}=0.001; p=0.974;$	
• Interaction		$F_{8,120}=1.463; p=0.177;$	
<i>DEVALUATION TEST</i>			
<b>Lever pressing</b>	WT	$4.753 \pm 1.469^{**}$	$w_{16}=-109.0; p=0.008; \text{Cohen's } d=0.785$
	LCN2-null	$3.272 \pm 2.332$	$w_{15}=-30.00 p=0.421$
<b>Normalized lever pressing</b>	WT	$0.355 \pm 0.106^{**}$	$w_{14}=-81.00; p=0.009; \text{Cohen's } d=0.864$
	LCN2-null	$0.002 \pm 0.074$	$w_{15}=16.00; p=0.706$

As predictable (Adams & Dickinson, 1981; Hilario, 2007), the actions of control mice became highly sensitive to sensory specific satiety (Figure 13C; Table 5). In fact, their responses significantly reduced when comparing the valued condition with the devalued one in the extinction test (see *Material and Methods*; Figure 13C; Table 5). Lever pressing was also normalized for the last day of RR20 training, to account for the baseline differences among animals (Figure 13C; Table 5). In contrast, LCN2-null mice became insensitive in their actions to the expected value assigned to the value of the reinforcers, as indicated in Figure 13C by a lack of devaluation effect (Table 5), meaning that, the animals developed a lever pressing habit that was maintained during the extinction test.

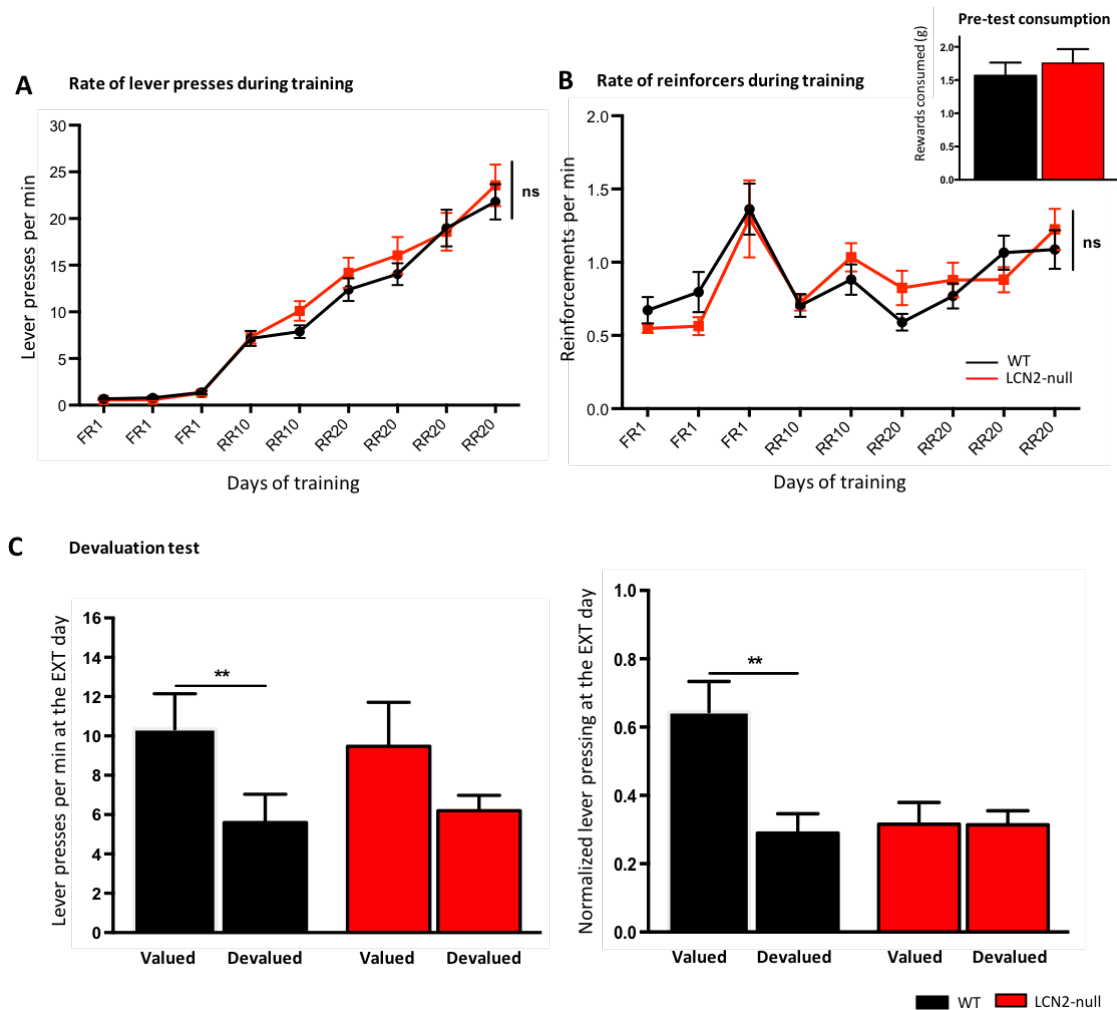


**Figure 13: LCN2-null mice presented a habitual lever pressing behavior when compared to the control group in an operant task.** (A) Acquisition of the lever pressing task in both groups. The rate of lever pressing is depicted for each daily session for the reward (pellets); (B) Rewards consumption was also controlled during training. The amount of rewards consumed by both groups during the ad libitum devaluation test days were also controlled; (C) Devaluation test analysis. Lever pressing in absolute number and normalized to the lever pressing of the last training day (RR20) is compared between the valued and the devalued condition for LCN2-null mice and WT littermate controls. Statistical analysis between groups for training curves was performed using two-way repeated measures ANOVA test, and Student's t-test for the extinction test. Two independent experiments were performed, and data is presented as mean  $\pm$  SEM (\*\* $p < 0.01$ ).

Overall, these data suggest that decision-making is biased in the absence of LCN2, predisposing LCN2-null mice to habitual behavioral strategies during instrumental training schedule.

#### 4.2 LCN2-null mice present excessive marble burying behavior

Multiple tests have been arising in the literature in the attempt to evaluate compulsive and anxious-like behaviors in mice that resemble OCD phenotype. Marble burying test is one example, which has been described to target a specific type of spontaneous behavior

observed in animals (Borsini, 2002; Deacon, 2006). The utility of the test for OCD-like behavior evaluation has already been reported by pharmacological evidences where marble burying was inhibited after anxiolytic benzodiazepine injections (Njung & Handley, 1991). Therefore, in line with the previous task, we then performed the marble burying test in LCN2-null mice along with their littermate controls.

For that, two independent experiments were performed and both groups were submitted to the test (n=8 mice per group). As it is illustrated in Figure 14A, 12 marbles were arrayed on the surface of clean bedding and the number of marbles buried in a 30 min session was scored by independent investigators blind to the genotype. Comparing both groups, LCN2-null mice buried roughly 69% of the marbles (on average correspond to 8 marbles buried), against 31% of the control group, which resemble in average only to 4 marbles buried (Figure 14B). This result indicates that the absence of LCN2 leads to a significant increasing of compulsive and anxious-like behaviors in mice (Table 6).

**Table 6: Statistical analysis of the marble burying test.** Data presented as mean  $\pm$  SEM, and statistical difference are reported as \*\* for  $p \leq 0.01$ .

	WT	LCN2-null	Statistical test, significance, effect size
# buried marbles	4.444 $\pm$ 1.042	8.333 $\pm$ 0.7638**	$t_{16}=3.01$ ; $p=0.0083$ ; Cohen's $d=4.257$

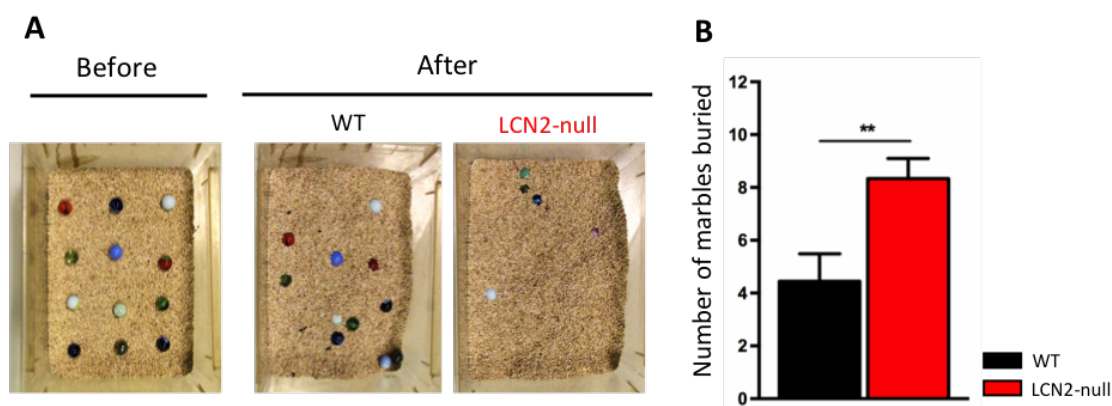


**Figure 14: LCN2-null mice display a compulsive and anxious phenotype in the marble burying test.** (A) Representative image of the field where mice performed the test, before and after (B) In a total of twelve marbles, LCN2-null mice buried significantly more when compared to the wild-type mice. Each bar shows the mean + SEM of 16 mice per group. Two independent experiments were performed and statistical analysis between groups was performed using Student's t-test (\*\*  $p < 0.01$ ).

### **4.3 Medium spiny neurons at the dorsomedial striatum are atrophic in the absence of LCN2**

After this striatal-dependent behavioral characterization and in an attempt to better understand the differences found, we went to look for striatal neuronal morphology. For that, we performed a Golgi-Cox staining analysis, specifically, at the DMS and DLS, which are critical areas at the striatum involved in habit learning and goal-directed formation (Kreitzer & Malenka, 2008).

As presented in Figure 15A, the absence of LCN2 caused an atrophy of the MSNs at the DMS, which is also translated into a significant reduction in the number of nodes when comparing to the WT mice. However, at the DLS subregion no major differences were found among genotypes in respect to total dendritic length and total number of nodes (Table 7). In addition, we also examined if LCN2 would be influencing spine density and morphology, by evaluating the percentage of each type of spines (Figure 15C, 15F, 15I, 15J). Overall, comparing LCN2-null mice with their littermate controls, no significant differences were found in both striatal areas (Table 7). Still, spine morphological composition analysis suggests that LCN2-null mice display an increased in thin spines and a decreased in mushroom spines, although it did not reach statistical significance (Table 7). In the sholl analysis, the number of intersections as a function of their distance from the soma, did not reveal any significant differences in LCN2-null mice, in DMS and DLS areas, when compared with WT (Figure 15G-H).

**Table 7: Statistical results of the morphological analysis comparing LCN2-null with wild-type mice in both DMS and DLS areas.** Data presented as mean  $\pm$  SEM for parametric tests, and as median  $\pm$  IQR for non-parametric tests. Statistical differences are reported as \* for  $p \leq 0.05$ , and \*\*\*\* for  $p \leq 0.0001$ .

<b>DMS</b>	<b>WT</b>	<b>LCN2-null</b>	<b>Statistical test, significance, effect size</b>
<b>Total dendritic length</b>	893.6 $\pm$ 50.31	748.3 $\pm$ 30.67 *	$t_{11}=2.363$ ; $p=0.038$ ; Cohen's $d=3.487$
<b>Number of nodes</b>	8.711 $\pm$ 0.463	6.966 $\pm$ 0.546 *	$t_{11}=2.392$ ; $p=0.036$ ; Cohen's $d=3.477$
<b>Spine density</b>	2.846 $\pm$ 0.146	2.624 $\pm$ 0.099	$t_{12}=1.257$ ; $p=0.233$
• Thin	19.23 $\pm$ 1.256	19.42 $\pm$ 1.053	$t_{12}=0.114$ ; $p=0.911$
• Mushroom	47.51 $\pm$ 5.402	43.26 $\pm$ 2.718	$t_{12}=0.702$ ; $p=0.496$
• Stubby	12.86 $\pm$ 1.591	12.47 $\pm$ 2.085	$t_{12}=0.149$ ; $p=0.884$
• Filopodia	9.266 $\pm$ 1.663	11.78 $\pm$ 1.327	U=15.00; $p=0.256$
• Detached	6.173 $\pm$ 2.034	9.604 $\pm$ 1.755	U=14.00; $p=0.207$
• Branched	4.969 $\pm$ 1.102	3.474 $\pm$ 0.637	$t_{12}=1.175$ ; $p=0.263$
<b>Sholl analysis</b>			
Genotype factor	$F_{1,12}=2.740$ ; $p=0.124$		
Interaction	$F_{9,108}=2.192$ ; $p=0.028$ ; $\eta^2=0.941$ *		
<b>DLS</b>			
<b>Total dendritic length</b>	937.3 $\pm$ 58.94	929.9 $\pm$ 32.54	$t_{12}=0.109$ ; $p=0.915$
<b>Number of nodes</b>	9.452 $\pm$ 0.455	8.387 $\pm$ 0.559	U=10.00; $p=0.065$
<b>Spine density</b>	2.807 $\pm$ 0.101	2.815 $\pm$ 0.120	U=23.50; $p=0.928$
• Thin	18.77 $\pm$ 1.532	22.36 $\pm$ 0.885	$t_{11}=1.938$ ; $p=0.079$
• Mushroom	52.40 $\pm$ 1.573	45.10 $\pm$ 3.103	$t_{11}=1.991$ ; $p=0.072$
• Stubby	13.28 $\pm$ 1.884	10.93 $\pm$ 1.958	$t_{12}=0.865$ ; $p=0.404$
• Filopodia	10.00 $\pm$ 1.090	12.64 $\pm$ 2.409	$t_{12}=0.996$ ; $p=0.339$
• Detached	7.023 $\pm$ 2.668	7.150 $\pm$ 1.191	U=16.00; $p=0.313$
• Branched	3.843 $\pm$ 0.790	2.661 $\pm$ 0.774	$t_{12}=1.068$ ; $p=0.306$
<b>Sholl analysis</b>			
Genotype factor	$F_{1,12}=0.267$ ; $p=0.615$ ; $\eta^2=0.0003$		
Interaction	$F_{9,108}=0.428$ ; $p=0.918$		



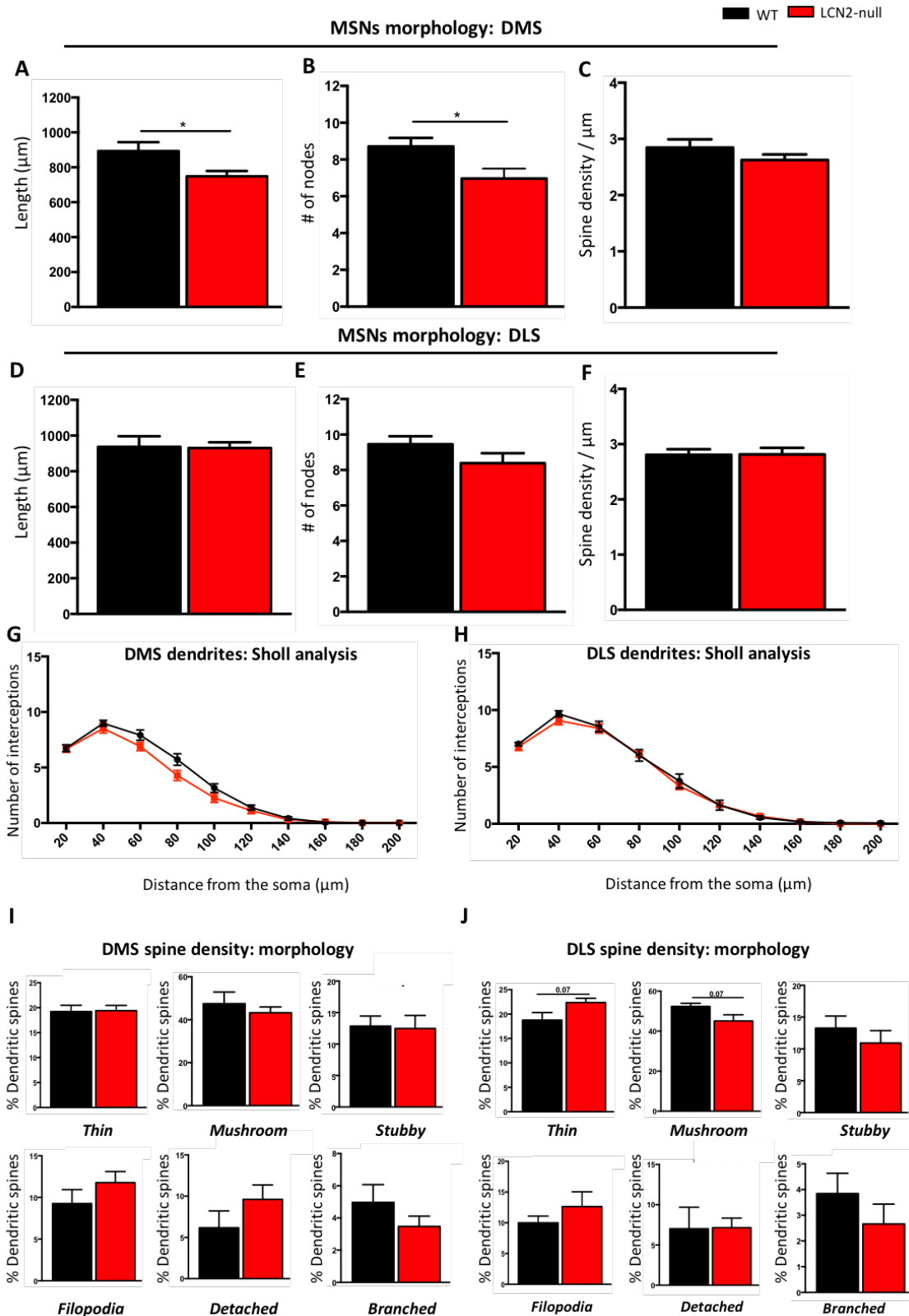


**Figure 15: Three-dimensional morphological analysis of Golgi-impregnated medium spine neurons (MSNs), of the dorsomedial (DMS) and dorsolateral striatum (DLS) reveals no major alterations by the absence of LCN2. (A) Total dendritic length (µm), (B) total number of nodes, and (C) spine density/µm, at the DMS. (D) Total dendritic length (µm), (E) total number of nodes, and (F) spine density/µm, at the DLS. Sholl analysis was also assessed at the (G) DMS and (H) DLS region. Spine morphology type was classified in both (I) DMS and (J) DLS areas. Each bar shows the mean ± SEM of**

one experiment with 7 mice per group. Statistical analysis between groups was performed using Student's t-test (\* $p < 0.05$ ). For Sholl analysis, curves represent mean  $\pm$  SEM, a two-way repeated-measures ANOVA test was used.

#### 4.4 Dorsomedial striatum neurons have lower amplitude of synaptic transmission in the absence of LCN2.

As previously showed, the absence of LCN2 have an impact in striatal-dependent behaviors, as well as, in MSNs morphology at the DMS. Therefore, and relying on the critical role of CSTC in the development of OCD pathophysiology (Saxena et al., 2000), we intend to extend our LCN2-null mice model characterization to the functional level. So, we performed whole-cell voltage clamp recordings of miniature excitatory postsynaptic currents (mEPSCs) in dorsomedial striatal MSNs.

In that sense, after behavioral tests, striatal slices were collected and used to registered electrophysiological recordings at the DMS. Compared to WT littermate controls, LCN2-null mice presented a significant reduction in mEPSC amplitude of synaptic transmission (Figure 16B; Table 8). On the other hand, no significant alternations at mEPSC frequency were found (Figure 16A; Table 8). Cumulative probability distribution (frequency and amplitude) was also compared in both genotype. As expected, a significant alteration in the distribution pattern of LCN2-null mice amplitude was found (Figure 16D; Table 8), while in the cumulative frequency were not (Figure 16C; Table 8).

**Table 8: Statistical analysis of electrophysiological recordings comparing LCN2-null mice with littermate controls.** Data presented as mean  $\pm$  SEM and, statistical difference are reported as \* for  $p \leq 0.05$ , and \*\*\*\* for  $p < 0.0001$ .

	WT	LCN2-null	Statistical test, significance, effect size
<b>mEPSC frequency</b>	1.937 $\pm$ 0.150	2.077 $\pm$ 0.196	$t_{26}=0.568$ ; $p=0.575$ ; Cohen's $d=0.801$
<b>mEPSC amplitude</b>	16.40 $\pm$ 0.505	14.77 $\pm$ 0.573*	$t_{26}=2.1829$ ; $p=0.043$ ; Cohen's $d=3.018$
<b>Cumulative frequency</b>			Kolmogorov-Smirnov $D=0.030$ ; $p=0.911$
<b>Cumulative amplitude</b>			Kolmogorov-Smirnov $D=0.154$ ; $p<0.0001$ ****

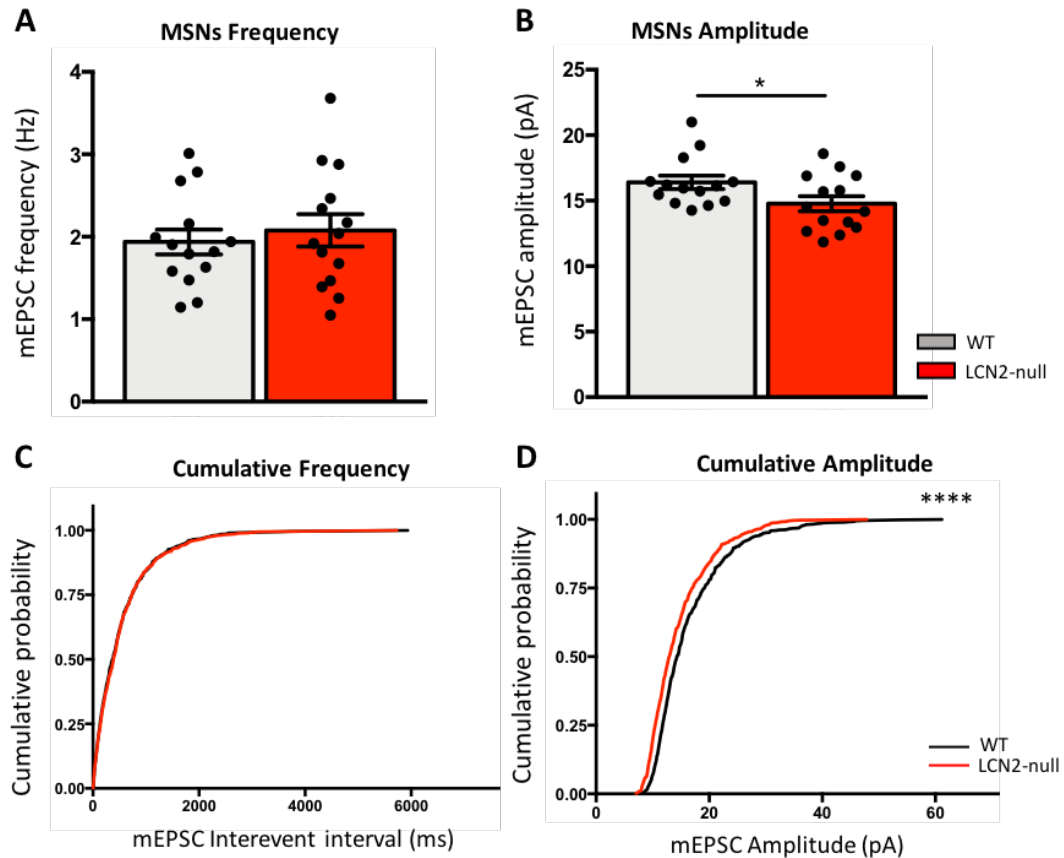


**Figure 16: Synaptic pattern in LCN2-null mice is not altered after behavioral tests in dorsomedial striatum medium spiny neurons.** (A) MSNs frequency and (B) amplitude in LCN2-null MSNs. (C) Cumulative probability distributions of mEPSC frequency showed no significant difference but (D) cumulative distribution of amplitude for LCN2-null mice was significantly altered when compared to WT mice (\* $p < 0.01$ , \*\*\*\*  $p < 0.0001$ ). Two-tailed t-test for mEPSC frequency and amplitude analysis. All data presented as mean  $\pm$  SEM and each bar represent one experiment with 3 mice per group. Statistical analysis between groups was performed using Student's t-test. Cumulative probability statistic was performed using the Kolmogorov-Smirnov test. Data contribution by Diana Rodrigues.

#### 4.5 Dorsomedial striatum neurons have lower amplitude of synaptic transmission in naïve LCN2-null mice.

After observing functional differences in LCN2-null mice amplitude, we questioned whether behavioral assessments could be influencing cortico-striatal synapses. To answer this question, we then performed mEPSCs recordings at the DMS (Figure 17A), but this time using young naïve LCN2-null mice.

Interestingly, we observed the same response as the previous described. Data analysis showed that LCN2-null mice presented no differences in the frequency (Figure 17B, Table 9), but displayed a reduced amplitude in the synaptic transmission (Figure 17C, Table 9), when compared to the WT mice. Also, the same pattern was registered at the cumulative probability distributions [frequency (Figure 17D, Table 9) and amplitude (Figure 17E, Table 9)].

**Table 9: Statistical analysis of electrophysiological recording comparing LCN2-null mice with littermate controls.** Data presented as mean  $\pm$  SEM and, statistical difference are reported as \* for  $p \leq 0.05$  and \*\*\*\* for  $p < 0.0001$ .

	WT	LCN2-null	Statistical test, significance, effect size
<b>mEPSC frequency</b>	2.446 $\pm$ 0.196	2.130 $\pm$ 0.299	$t_{22}=0.883$ ; $p=0.387$ ; Cohen's $d=1.249$
<b>mEPSC amplitude</b>	17.62 $\pm$ 0.676	15.90 $\pm$ 0.416*	$t_{22}=2.160$ ; $p=0.042$ ; Cohen's $d=3.065$
<b>Cumulative frequency</b>			Kolmogorov-Smirnov $D=0.068$ ; $p=0.102$
<b>Cumulative amplitude</b>			Kolmogorov-Smirnov $D=0.142$ ; $p<0.0001$ ****

## A MSNs electrophysiology records

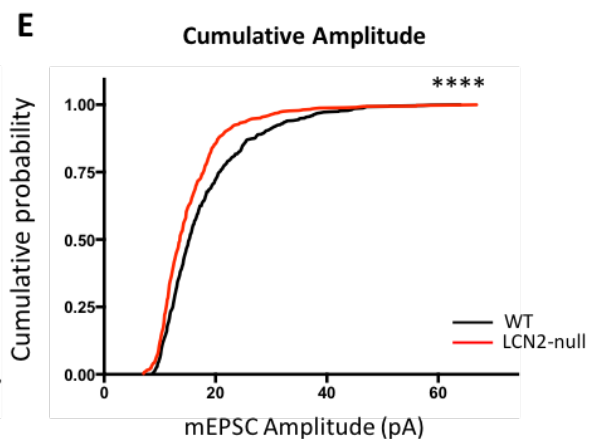
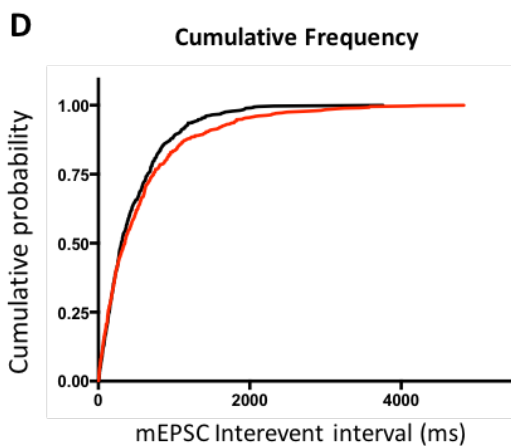
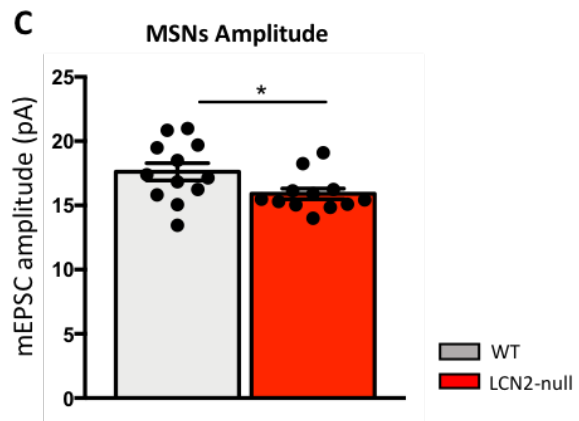
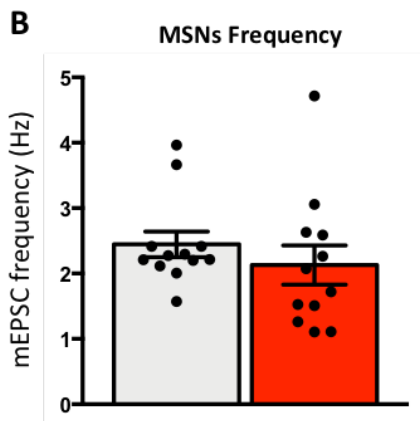
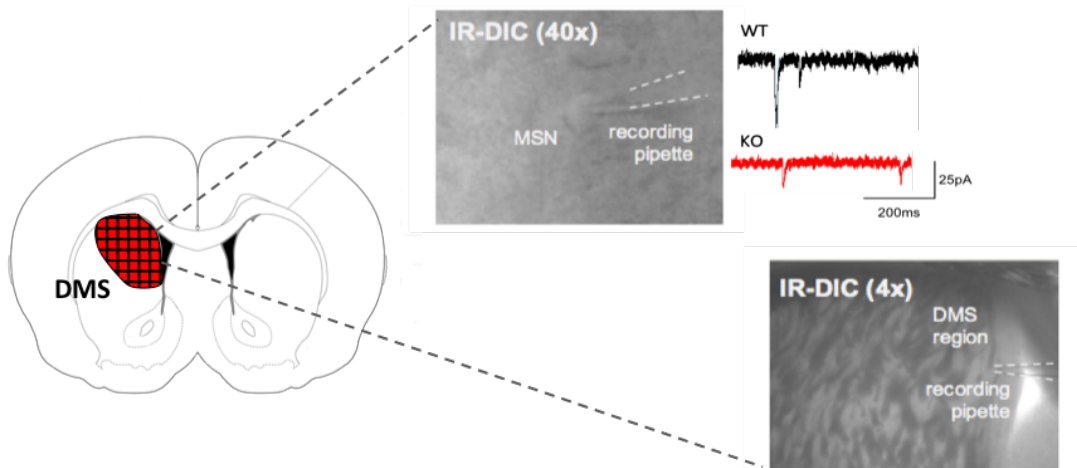


**Figure 17: LCN2-null mice displayed reduced amplitude of excitatory synaptic transmission in dorsomedial striatum medium spiny neurons.** (A) IR-DIC images from the recording neuron (4x and 40x) and mEPSC example traces from control and LCN2-null mice, recorded with whole-cell voltage clamp from striatal medium spiny neurons. (B) No significant alterations were found in the mEPSC frequency, but a (C) reduced amplitude was detected in LCN2-null MSNs. (D) Cumulative probability distributions of mEPSC frequency showed no significant difference but (E) cumulative distribution of amplitude for LCN2-null mice was significantly altered when compared to WT mice (\* $p < 0.01$ , \*\*\*\*  $p < 0.0001$ ). Two-tailed t-test for mEPSC frequency and amplitude analysis. All data presented as mean  $\pm$  SEM and each bar represent one experiment with 3 mice per group. Statistical analysis between groups was performed using Student's t-test. Cumulative probability statistic was performed using the Kolmogorov-Smirnov test. Data contribution by Patrícia Monteiro.

Overall, electrophysiological analysis uncovered basal defects at striatal synapses in LCN2-null mice regarding synaptic amplitude. These findings suggest a physiological role for LCN2 in postsynaptic functioning and connectivity at the CSTC.

#### **4.6 The absence of LCN2 induces increased *Psd-95* gene expression**

Having in mind the results obtained specially, in the electrophysiology for LCN2-null mice, we next questioned if synaptic gene expression was also altered in the striatum. For that, our first approach was to assess gene expression levels of a selected group of synaptic proteins and receptors, that could be involved in the synaptic alterations registered in the electrophysiological data (Table 3– see Materials and Methods).

No major differences were found between LCN2-null mice and their littermate controls regarding synaptic gene expression (Figure 18, Table 10). However, as it is observed in Figure 18G, *Psd-95*, a major scaffolding postsynaptic protein (Cho et al., 1992), was significantly increased in the striatum of LCN2-null mice.

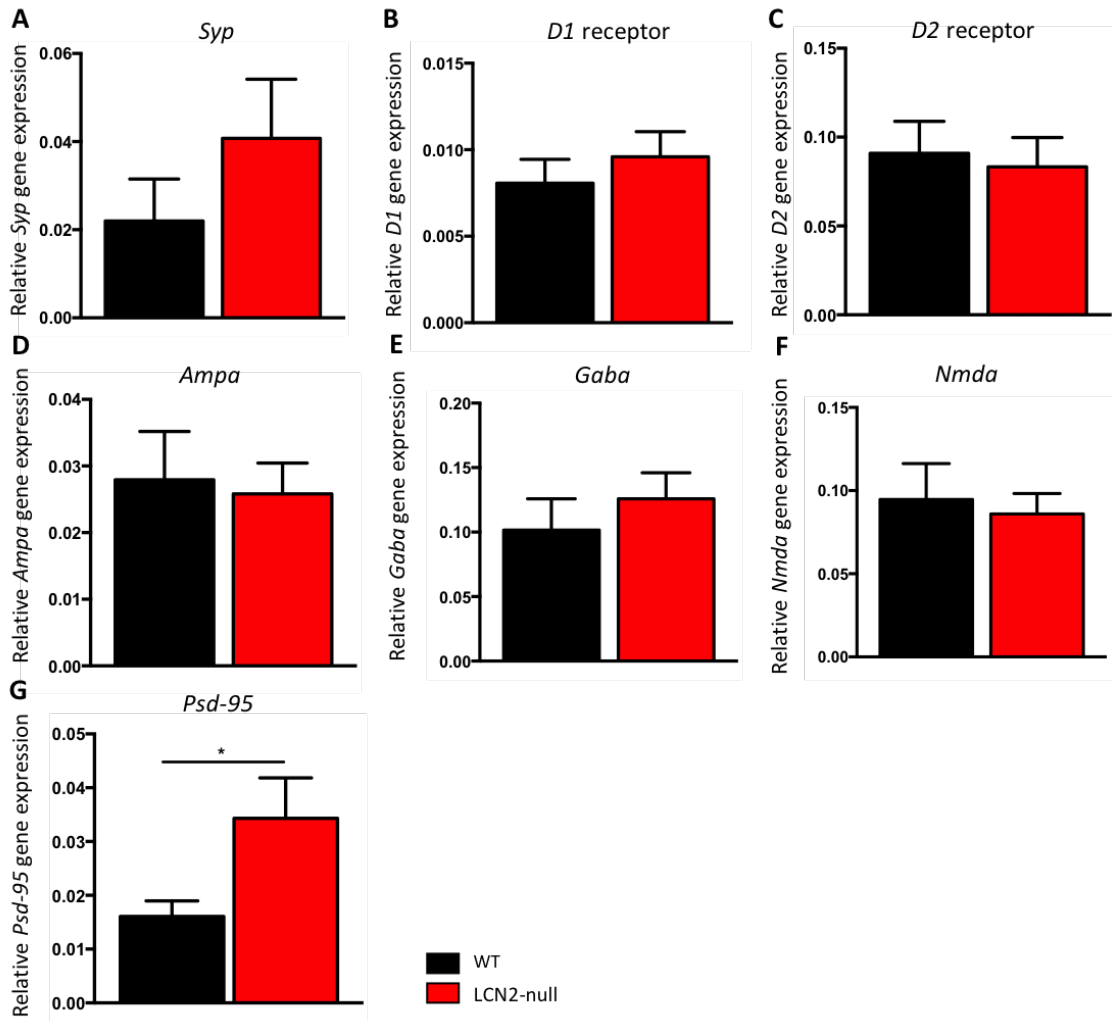


**Figure 18: LCN2 absence does not induce major differences in striatal gene expression.** RNA from striatum was extracted and transcribed to cDNA and the expression of (A) *Syp*, (B) *D1 receptor*, (C) *D2 receptor*, (D) *Ampa*, (E) *Gaba*, (F) *Nmda* and (G) *Psd-95* was accessed by qRT-PCR. Relative expression of each gene was normalized to the expression of *Atp5b* and *Hspcb* housekeeping genes. Data is show as mean  $\pm$  SEM from one experiment with 8 mice per group (only for *Psd-95* evaluation was used a group of  $n_{WT}=16$  and  $n_{LCN2-null}=16$ ). Statistical analysis between groups was performed using Student's t-test (\*  $p < 0.05$ ).

Further, and considering our theoretical hypothesis, we also analyzed the expression of some specific genes that are particularly interesting in this context, such as the *Mc4r*, *Sapap3* and *Shank3*. As it was previously mentioned, MC4R has been pointed as an important mediator for compulsive behaviors in animals (Xu et al., 2013), and also as a novel receptor for LCN2 (Mosialou et al., 2017b). Additionally, *Sapap3* and *Shank3* were assessed due to their involvement in OCD-mouse model and striatal dysfunction (Peça et al., 2011; Wan et al., 2014; Xu et al., 2013). Therefore, we also performed a qRT-PCR to evaluate their expression at the striatum and, depicted in Figure 19 no significant alterations were found between genotypes (Table 10).

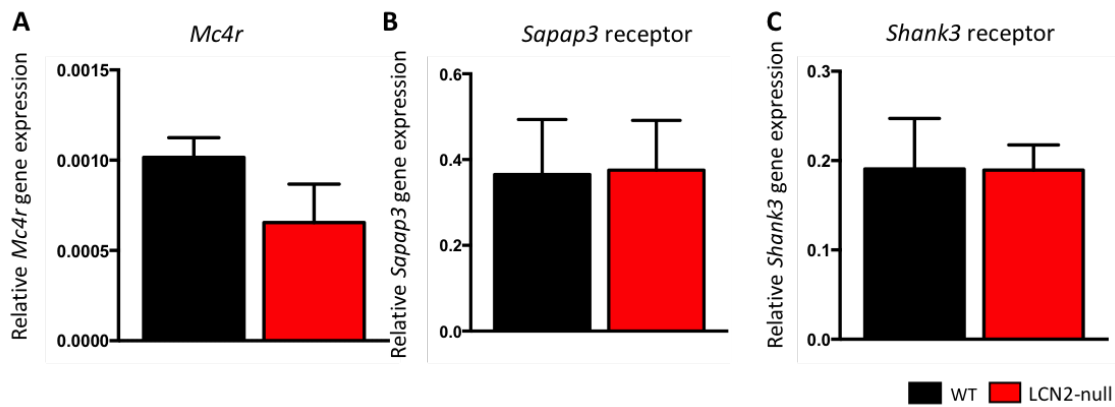


**Figure 19: Differential expression of specific gene markers in the striatum.** RNA from striatum was extracted and transcribed to cDNA and the expression of (A) *Mc4r*, (B) *Sapap3*, and (C) *Shank3* was accessed by qRT-PCR. Relative expression of each gene was normalized to the expression of *Atp5b* and *Hspcb* housekeeping genes. Data are represented as the mean  $\pm$  SEM of one experiment with 8 mice per group. Statistical analysis between groups was performed using Student's t-test.

**Table 10: Statistical analysis regarding relative gene expression in the striatum.** Data presented as mean  $\pm$  SEM for parametric tests, and as median  $\pm$  IQR for non-parametric tests. Statistical difference is reported as \* for  $p \leq 0.05$ .

Target gene	WT	LCN2-null	Statistical test, significance, effect size
<i>Syp</i>	0.031 $\pm$ 0.013	0.056 $\pm$ 0.018	U=13.00; $p=0.289$
<i>D1 receptor</i>	0.008 $\pm$ 0.001	0.009 $\pm$ 0.001	U=69.00; $p=0.892$
<i>D2 receptor</i>	0.091 $\pm$ 0.018	0.083 $\pm$ 0.017	$t_{12}=0.311$ ; $p=0.7613$
<i>Ampa</i>	0.028 $\pm$ 0.007	0.026 $\pm$ 0.005	$t_{12}=0.247$ ; $p=0.809$
<i>Gaba</i>	0.102 $\pm$ 0.024	0.126 $\pm$ 0.020	$t_{12}=0.772$ ; $p=0.455$
<i>Nmda</i>	0.095 $\pm$ 0.022	0.086 $\pm$ 0.012	$t_{12}=0.349$ ; $p=0.734$
<i>Psd-95</i>	0.016 $\pm$ 0.003	0.034 $\pm$ 0.008*	$t_{20}=2.259$ ; $p=0.035$ ; Cohen's $d=3.194$
<i>Mc4r</i>	0.001 $\pm$ 0.0001	0.001 $\pm$ 0.0002	$t_{12}=1.507$ ; $p=0.158$
<i>Sapap3</i>	0.014 $\pm$ 0.009	0.011 $\pm$ 0.009	U=67.00; $p=0.804$
<i>Shank3</i>	0.191 $\pm$ 0.057	0.189 $\pm$ 0.028	U=46.00; $p=0.148$

Overall, LCN2 absence does not modulate the expression of the striatal genes tested, associated both with synaptic modulation and striatal markers, with the exception of *Psd-95* gene expression.



**CHAPTER 5**

---

**5. DISCUSSION**



Over the past few years, LCN2 has been described to be involved in a wide range of pathophysiological conditions from immunological deficits to impairments in the CNS (Ferreira et al., 2015). In the brain, although the emergent state of the art, the role and impact of LCN2 remains unclear. Interestingly, Mosialou *et al.* (2007) reported MC4R as a novel LCN2 receptor in the paraventricular and ventromedial neurons of the hypothalamus, thus evoking a new molecular pathway for LCN2 (Mosialou et al., 2017). Of relevance, it was shown that when LCN2 binds to MC4R, this resulted in altered food intake behaviors, which is a type of compulsive behavior. Additionally, it was demonstrated that MC4R gene deletion is able to rescue compulsive behaviors in animal models of human OCD (Xu et al., 2017) (Figure 7). However, the underlying mechanism remains unknown. These findings have raised the question if this can be mediated by its ligand LCN2. So, herein, we aim to give study whether LCN2 is regulating compulsive behaviors in the striatum through MC4R.

Based on our proposal, our initial aim was to explore LCN2-null mice striatal-dependent behaviors. Throughout our experiments, we have focused only on mice males in order to reduce the heterogeneity usually associated with female hormonal status (Aoki et al., 2010). First, we performed an operant conditioning test in a random-ratio interval, to assess decision-making in animals. Interestingly, LCN2-null mice developed a habit-based strategy during the devaluation test, meaning that the absence of LCN2 is somehow impairing goal-directed behavior in mice (Figure 20). Moreover, upon the marble burying test, LCN2-null mice displayed an increased burying when compared to the WT littermate controls, evoking a compulsive and anxious-like behaviors in LCN2-null mice (Figure 20). In accordance, previous studies from *Ferreira et al.*, (2013) have shown that LCN2-null mice display anxious and depressive-like behaviors, as well as cognitive impairments (Ferreira et al., 2013). Although we need to better characterize these animals in terms of their decision-making behavioral, herein we cannot exclude that the already described anxious-like behavior observed in LCN2-null mice might have some influence in goal-directed action in these animals. In fact, goal-directed behaviors encode for a strict link between an action and an objective, and the fact that LCN2-null are more anxious could be altering this relationship. Moreover, the emotional alterations reported in LCN2-null

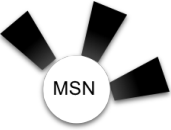




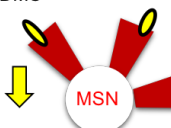
mice could also be affecting the exploration rate activity of animals during the operant conditioning test, decreasing their sensibility to the devaluation test.

Once a putative role for LCN2 has been emerged in mediating compulsive and anxious-like behavior in mice, we also looked for morphological and functional striatal features in LCN2-null mice.

Since decision-making is mainly mediated by the DMS and DLS (Hilario et al., 2008), we started by analyzing if LCN2 could be affecting MSNs three-dimensional morphology in both regions. Regarding the morphometric data, the absence of LCN2 had led to a significant atrophy of MSNs at the DMS, the same area that is involved in supporting goal-directed actions (Figure 20). Further, we also evaluated striatal synaptic functioning at the DMS through electrophysiological records. To better understand the physiological role of LCN2 in synaptic transmission at the DMS, electrophysiological recordings were performed in two different experiments: first, in animals that performed behavioral assessments; and, second, in naïve LCN2-null and WT mice. Remarkably, both results were similar, evoking a critical role for LCN2 in basal conditions at the DMS (Figure 20). In fact, the absence of LCN2 had led to a reduction in mEPSC amplitude, indicating a reduction in the total number of receptors per spine in MSNs. Moreover, mEPSC frequency was not altered, meaning that the absence of LCN2 does not compromised the number of mature spines in MSNs.

Finally, molecular analysis was also assessed in order to determine if relative striatal gene expression in LCN2-null mice would be affected. Over a wide screening of genes, we observed that *Psd-95* was significantly up-regulated in the striatum of LCN2-null mice. PSD-95 is an important scaffolding protein required to molecular organization of the postsynaptic density, by sustaining different types of receptors, cytoskeletal proteins, and signaling molecules (El-Hussein et al., 2000). Further, as an important protein involved in postsynaptic spines, it would be speculated that a higher *Psd-95* expression could be related with a higher number of spines, leading to increased mEPSC frequency; however, this relationship was not observed in our results. This could be due to fact that, *Psd-95* was assessed in the whole striatum without DMS and DLS division, which would be an important assessment to perform in a near future. Additionally, it is also important to have

in mind that mRNA *Psd-95* expression may not be totally translated into functional protein. Then, to better understand the potential impact of this scaffolding protein in the LCN2-null striatum mice, it is crucial in future experiments to determine PSD-95 protein expression through Western Bolt.

	WT mice		LCN2-null mice	
<b>Operant conditioning test</b>	Goal-directed actions		Habit-based actions	
<b>Marble burying test</b>	Normal phenotype		Compulsive and anxious-like phenotype	
<b>Morphological analysis</b>	DMS 	DLS 	DMS 	DLS 
<b>Electrophysiology data</b>	DMS 	DLS ?	DMS 	DLS ?
<b>Gene expression analysis</b>	Striatal genes analysis: <i>Syp, D1, D2, Ampa, Gaba, Nmda, Psd-95, Shank3, Mc4r and Sapap3.</i>		Increased <i>Psd-95</i> expression	

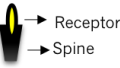


**Figure 20: Schematic overview of the observed LCN2-null mice phenotype.** LCN2-null mice were compared to their WT littermate controls in different tasks, with different proposes, since behavioral characterization to morphological and functional analysis.

In fact, as it is illustrated in Figure 21, we showed that the absence of LCN2 expression led to compulsive and anxious-like behaviors in mice, which resemble OCD phenotype. Further, we also showed that the absence of LCN2 leads to morphological and functional alterations at the dorsal striatum. Regarding Xu *et al.*, (2013) work's, we know that SAPAP3-null mice, a well-characterized OCD-mouse model, normalize their behavioral and electrophysiological impairments after genetic deletion of MC4R (Xu et al., 2013). As a result, it is suggested that MC4R expression can be also an important mediator in the promotion of compulsive behaviors in mice.

Linking all these evidence, one plausible possibility is that the absence of LCN2, a ligand for MC4R, might be triggering MC4R over expression in the brain; and in turn, MC4R over expression results in OCD-like behaviors observed in LCN2-null mice (Figure 21).

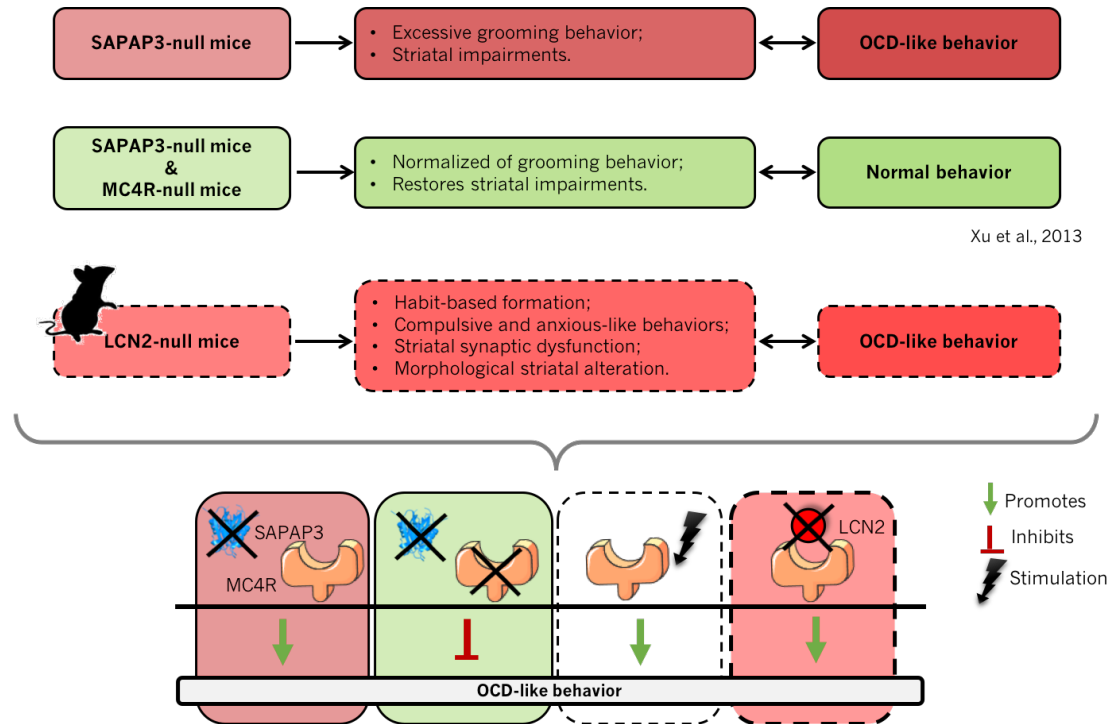


**Figure 21: Hypothetical role for LCN2 in the involvement of OCD-like behaviors.** SAPAP3-null mice are a well-characterized OCD-mice model, displaying excessive grooming behavior and striatal impairments. Previous studies from Xu et al., (2013) have shown that double deletion of SAPAP3 and MC4R leads to a normalization of grooming behavior in mice, as well as, a restore in striatal synaptic impairments. Regarding our work, in this thesis we showed that LCN2-null mice display a habitual behavior, as an increase compulsivity and anxious-like behavior. Nevertheless, we also showed that the absence of LCN2 had led to morphological alterations and synaptic dysfunction, in the striatum. Therefore, based on Xu et al., (2013) work, we hypothesize a role for MC4R in mediating OCD-like behaviors, which can also be involved in in the phenotype observed in LCN2-null mice.

To test this hypothesis, we assessed the levels of *Mc4r*, as well as, other striatal genes of interest, such as, *Sapap3* and *Shank3*, owing their major characteristic in striatal functioning and OCD. It would be expected that *Mc4r* gene expression would be increased in LCN2-null mice. Although we did not find evidence of increased *Mc4r* expression in striatum, mRNA analysis is not sufficient to assess the amount of this receptor and its presence in the cell membrane. In fact, post-transcriptional processes are key to the final syntheses of the functional protein. For instance, despite high gene expression, the receptor can be confined to vesicles and not be expressed in the cellular membranes. Also, it is important to have in mind that striatum might just be an

intermediated region, that MC4R could be inducing its effects in other brain regions, for instance, in the hypothalamus.

Overall, a putative role for LCN2 in mediating compulsive and striatal-dependent behaviors, and striatal modulation has been emerged. Considering our main hypothesis we can speculate a novel involvement of LCN2 in OCD-like behaviours.





## CHAPTER 6

---

### 6. FINAL REMARKS



Altogether, some interesting insights about the role of LCN2 in the striatum have been addressed and a new feature for LCN2 in the mediation of OCD-like behaviors has been speculated. With this thesis we can conclude that:

- i) The absence of LCN2 impairs goal-directed action and leads to a compulsive and anxious-like behaviours in mice;
- ii) The neurons from the brain region involved in supporting goal-directed actions (DMS) is altered in LCN2-null mice: neurons were atrophic and mEPSCs amplitude was reduced;
- iii) Finally, LCN2-null mice display an increasing of *Psd-95* expression in the striatum.

Therefore, since in this work it was only performed an initial step in the long run to better understand and explore the impact of LCN2 in the striatal function and their relation with MC4R, it is important, in a near future, to answer some additional questions.

- i) Synaptic dysfunction was observed at the DMS, but how is LCN2 modulating synaptic activity at the DLS?
- ii) Similarly, to the fundamental behind electrophysiological data, is behavioral assessments affecting MSNs morphology?
- iii) Could *Psd-95* be correlated with PSD-95 protein expression? And, at the DMS and DLS?
- iv) Although the results regarding the *Mc4r* expression in LCN2-null mice, could MC4R protein levels be different? And, can MC4R be differently expressed in different brain regions of LCN2-null mice?

These and many other underlying questions are the ones we pretend to, in a near future, answer. Globally, we pretend to clarify the role of LCN2 in physiological striatum functioning and how this protein could be mediating the MC4R-signaling pathway in SAPAP3-null mice.



**CHAPTER 7**

---

**7. REFERENCES**



- Adams, C.D. & Dickinson, A. (1981). Instrumental responding following reinforcer devaluation. *The Quarterly Journal of Experimental Psychology*, 33(2), 109–121.
- Adams, P.C., Barton, J.C., Guo, H., Alter, D. & Speechley, M. (2015). Serum ferritin is a biomarker for liver mortality in the hemochromatosis and iron overload screening study. *Annals of Hepatology*, 14(3), 348–353.
- Adams, T.G., Kelmendi, B., Brake, C.A., Gruner, P., Badour, C.L. & Pittenger, C. (2018). The role of stress in the pathogenesis and maintenance of Obsessive-Compulsive Disorder. *Chronic Stress*, 2(1), 1-11.
- Adan, R.A.H., Tiesjema, B., Hillebrand, J.J.G., La Fleur, S.E., Kas, M.J.H. & De Krom, M. (2006). The MC4 receptor and control of appetite. *British Journal of Pharmacology*, 149(7), 815–827.
- Ahmari, S.E., Spellman, T., Douglass, N.L., Kheirbek, M.A., Simpson, H.B., Deisseroth, K. & Hen, R. (2013). Repeated cortico-striatal stimulation generates persistent OCD-like behavior. *Science*, 340(6137), 1234–1239.
- Aigner, F., Maier, H.T., Schwelberger, HG., Wallnöfer, E.A., Amberger, A., Obrist, P., Mak, T.W, Maglione, M., Margreiter, R., Schneeberger, S. & Troppmair, J. (2007). Lipocalin-2 regulates the inflammatory response during ischemia and reperfusion of the transplanted heart. *American Journal of Transplantation*, 7(4), 779–788.
- Alvaro, J.D., Taylor, J.R & Duman, R.S. (2003). Molecular and behavioral interactions between central melanocortins and cocaine. *The Journal of Pharmacology and Experimental Therapeutics*, 304(1), 391–399.
- Aoki, M., Shimozuru, M., Kikusui, T., Takeuchi, Y. & Mori, Y. (2010) Sex differences in behavioral and corticosterone responses to mild stressors in ICR mice are altered by ovariectomy in peripubertal period. *Zoolog Science*, 27(10), 783-789.
- Aosaki, T., Miura, M., Suzuki, T., Nishimura, K. & Masuda, M. (2010). Acetylcholine-dopamine balance hypothesis in the striatum: An update. *Geriatrics and Gerontology International*, 10(1), 148-157.
- APA. (2013). *American Psychiatric Association: statistical Manual of Mental Disorders (DSM-5)*. Lake St. Louis, MO.
- Arnold, P.D., Sicard, T., Burroughs, E., Richter, M.A. & Kennedy, J.L. (2006). Glutamate transporter gene *SLC1A1* associated with obsessive-compulsive disorder. *Archives of General Psychiatry*, 63(7), 769–776.
- Arosio, P., Elia, L. & Poli, M. (2017). Ferritin, cellular iron storage and regulation. *IUBMB Life*, 69(6), 414–422.
- Atallah, H.E., Lopez-Paniagua, D., Rudy, J.W. & O'Reilly, R.C. (2007). Separate neural substrates for skill learning and performance in the ventral and dorsal striatum. *Nature Neuroscience*, 10(1), 126–131.

- Ataseven, A., Kesli, R., Kurtipek, G.S. & Ozturk, P. (2014). Assessment of lipocalin-2, clusterin, soluble tumor necrosis factor receptor-1, interleukin-6, homocysteine, and uric acid levels in patients with psoriasis. *Disease Markers*, 2014 (2014), 1-7.
- Bachman, M.A., Miller, V.L. & Weiser, J.N. (2009). Mucosal lipocalin-2 has pro-inflammatory and iron-sequestering effects in response to bacterial enterobactin. *PLoS ONE Pathogens*, 5(10), 1-11.
- Balleine, B.W., Delgado, M.R. & Hikosaka, O. (2007). The role of the dorsal striatum in reward and decision-making. *Journal of Neuroscience*, 27(31), 8161–8165.
- Balthasar, N., Dalgaard, L.T., Lee, C.E., Yu, J., Funahashi, H., Williams, T., Ferreira, M., Tang, V., McGovern, R.A., Kenny, C.D., Christiansen, L.M., Edelman, E., Choi, B., Boss, O., Aschkenasi, C., Zhang, C.Y., Mountjoy, K., Kishi, T., Elmquist, J.K. & Lowell, B.B. (2005). Divergence of melanocortin pathways in the control of food intake and energy expenditure. *Cell*, 123(3), 493–505.
- Bao, G.H., Ho, C.T. & Barasch, J. (2015). The ligands of Neutrophil Gelatinase-Associated Lipocalin. *Royal Society of Chemistry Advances*, 5(126), 104363–104374.
- Bao, G., Clifton, M., Hoette, T.M., Mori, K., Deng, S., Qiu, A., Viltard, M., Williams, D., Paragas, N., Leete, T., Kulkarni, R., Li, X., Lee, B., Kalandadze, A., Ratner, A.J., Pizarro, J.C., Schmidt-Ott, K.M., Landry, D.W., Raymond, K.N., Roland, K.S. & Barasch, J. (2010). Iron traffics in circulation bound to a siderocalin (Ngal)-catechol complex. *Nature Chemical Biology*, 6(8), 602–609.
- Berger, T., Togawa, A., Duncan, G.S., Elia, A.J., You-Ten, A., Wakeham, A., Fong, H.E., Cheung, C.C. & Mak, T.W. (2006). Lipocalin-2-deficient mice exhibit increased sensitivity to *Escherichia coli* infection but not to ischemia-reperfusion injury. *Proceedings of the National Academy of Sciences of the USA*, 103(6), 1834–1839.
- Bertran-Gonzalez, J., Hervé, D., Girault, J.A. & Valjent, E. (2010) What is the degree of segregation between striatonigral and striatopallidal projections? *Frontiers in Neuroanatomy*, 136(4), 1-9.
- Boedhoe, P. S. W., Schmaal, L., Abe, Y., Ameis, S.H., Arnold, P.D., Batistuzzo, M.C., Benedetti F., Beucke J.C., Bollettini, I., Bose, A., Brem, S., Calvo, A., Cheng, Y., Cho, K.I., Dallspezia, S., Denys, D., Fitzgerald, K.D., Fouche, J.P., Giménez, M., Gruner, P., Hanna, G.L., Hibar, D.P., Hoexter, M.Q., Hu, H., Huyser, C., Ikari, K., Jahanshad, N., Kathmann, N., Kaufmann, C., Koch, K., Kwon, J.S., Lazaro, L., Liu Y., Lochner, C., Marsh, R., Mataix-Cols, D., Menchón, J.M., Minuzzi, L., Nakamae, T., Nakao, T., Narayanaswamy, J.C., Piras, F., Pittenger, C., Reddy, Y.C., Sato, J.R., Simpson, H.B., Soreni, N., Soriano-Mas, C., Spalletta, G., Stevens, M.C., Szeszko, P.R., Tolin, D.F., Venkatasubramanian, G., Walitza, S., Wang, Z., van Wingen, G.A., Xu, J., Xu, X., Yun, J.Y., Zhao, Q., Thompson, P.M., Stein, D.J. & van den Heuvel, O.A. (2017). Distinct subcortical volume alterations in pediatric and adult OCD: A worldwide meta- and mega-analysis. *American Journal of Psychiatry*, 174(1), 60–70.



- Bolze, F. & Klingenspor, M. (2009). Mouse models for the central melanocortin system. *Genes and Nutrition*, 4(2), 129–134.
- Borsini, F., Podhorna, J. & Marazziti, D. (2002). Do animal models of anxiety predict anxiolytic-like effects of antidepressants? *Psychopharmacology*, 163(2), 121–141.
- Burguière, E., Monteiro, P., Mallet, L., Feng, G. & Graybiel, A.M. (2008). Striatal circuits, habits, and implications for obsessive-compulsive disorder. *Growth*, 23(1), 1–7.
- Camaschella, C. (2015). Iron-deficiency anemia. *New England Journal of Medicine*, 372(19), 1832–1843.
- Caza, M. & Kronstad, J.W. (2013). Shared and distinct mechanisms of iron acquisition by bacterial and fungal pathogens of humans. *Frontiers in Cellular and Infection Microbiology*, 3(80), 1–23.
- Chia, W.J., Dawe, G.S. & Ong, W.Y. (2011). Expression and localization of the iron-siderophore binding protein lipocalin-2 in the normal rat brain and after kainate-induced excitotoxicity. *Neurochemistry International*, 59(5), 591–599.
- Cho, K.O., Hunt, C.A. & Kennedy, M.B. (1992). The rat brain postsynaptic density fraction contains a homolog of the drosophila discs-large tumor suppressor protein. *Neuron*, 9(5), 929–942.
- Christensen, E.I. & Birn, H. (2002). Megalin and cubilin: Multifunctional endocytic receptors. *Nature Reviews Molecular Cell Biology*, 3(4), 258–268.
- Chu, S.T., Lin, H.J., Huang, H.L. & Chen, Y.H. (1998). The hydrophobic pocket of 24p3 protein from mouse uterine luminal fluid: Fatty acid and retinol binding activity and predicted structural similarity to lipocalins. *The Journal of Peptide Research*, 52(4), 390–397.
- Cowland, J.B. & Borregaard, N. (1997). Molecular characterization and pattern of tissue expression of the gene for neutrophil gelatinase-associated lipocalin from humans. *Genomic*, 45(1), 17–23.
- Cui, H., Mason, B.L., Lee, C., Nishi, A., Elmquist, J.K. & Lutter, M. (2012). Neurons are required for procedural memory learning. *Physiology & Behavior*, 106(2), 201–210.
- De Biase, A., Knobloch, S.M., Di Giovanni, S., Fan, C., Molon, A., Hoffman, E.P. & Faden, A.I. (2005). Gene expression profiling of experimental traumatic spinal cord injury as a function of distance from impact site and injury severity. *Physiological Genomics*, 22(3), 368–381.
- Deacon, R.M.J. (2006). Digging and marble burying in mice: Simple methods for *in vivo* identification of biological impacts. *Nature Protocols*, 1(1), 122–124.
- Devireddy, L.R., Gazin, C., Zhu, X. & Green, M.R. (2005). A cell-surface receptor for

- lipocalin 24p3 selectively mediates apoptosis and iron uptake. *Cell*, 123(7), 1293–1305.
- Devireddy, L.R., Hart, D.O., Goetz, D. & Green, M.R. (2010). A mammalian siderophore synthesized by an enzyme with a bacterial homologue involved in enterobactin production. *Cell*, 141(6), 1006–1017.
- Dias-Ferreira, E., Sousa, J.C., Melo, I., Morgado, P., Mesquita, A.R., Cerqueira, J.J., Costa, R.M. & Sousa, N. (2009). Chronic stress causes frontostriatal reorganization and affects decision-making. *Science*, 325(625), 621–625.
- Dickinson, A. (1985). Actions and Habits: The development of behavioural autonomy. *Philosophical Transactions of the Royal Society: Biological Sciences*, 308(1135), 67–78.
- Ding, L., Hanawa, H., Ota, Y., Hasegawa, G., Hao, K., Asami, F., Watanabe, R., Yoshida, T., Toba, K., Yoshida, K., Ogura, M., Kodama, M. & Aizawa, Y. (2010). Lipocalin-2/neutrophil gelatinase-B associated lipocalin is strongly induced in hearts of rats with autoimmune myocarditis and in human myocarditis. *Circulation Journal*, 74(3), 523–530.
- El-Hussein, A., Schnell, E., Chetkovich, D.M., Nicoll, R.A. & Brecht, D.S. (2000). PSD-95 involvement in maturation of excitatory synapses. *Science*, 290(3), 1364–1368.
- Farooqi, I.S. & O’Rahilly, S. (2008). Mutations in ligands and receptors of the leptin-melanocortin pathway that lead to obesity. *Nature Clinical Practice Endocrinology and Metabolism*, 4(10), 569–577.
- Ferreira, A., Pinto, V., Mesquita, S.D., Novais, A., Sousa, J.C., Correia-Neves, M., Sousa, N., Palha, J.A. & Marques, F. (2013). Lipocalin-2 is involved in emotional behaviors and cognitive function. *Frontiers in Cellular Neuroscience*, 7(122), 1–10.
- Ferreira, A., Mesquita, S.D., Sousa, J.C., Correia-Neves, M., Sousa, N., Palha, J.A. & Marques, F. (2015). From the periphery to the brain: Lipocalin-2, a friend or a foe? *Progress in Neurobiology*, 131(7), 120–136.
- Ferreira, A.C., Santos, T., Sampaio-Marques, B., Novais, A., Mesquita, S.D., Ludovico, P., Bernardino, L., Correia-neves, M, Sousa, N., Palha, J.A., Sousa, J.C. & Marques, F. (2018). Lipocalin-2 regulates adult neurogenesis and contextual discriminative behaviours. *Molecular Psychiatry*, 23(4), 1–9.
- Flo, T., Smith, K. & Sato, S. (2004). Lipocalin-2 mediates an innate immune response to bacterial infection by sequestering iron. *Nature*, 432(7019), 917–921.
- Flower, D.R. (1996). The lipocalin protein family: Structure and function. *The Biochemical Journal*, 318(1), 1–14.
- Flower, D.R., North, A.C.T. & Sansom, C.E. (2000). The lipocalin protein family: Structural and sequence overview. *Biochimica et Biophysica Acta - Protein*

*Structure and Molecular Enzymology*, 1482(2), 9–24.

- Fogel, J. (2003). An epidemiological perspective of obsessive-compulsive disorder in children and adolescents. *The Canadian Child and Adolescent Psychiatry Review*, 12(2), 33–36.
- Friedl, A., Stoesz, S.P., Buckley, P. & Gould, M.N. (1999). Neutrophil gelatinase-associated lipocalin in normal and neoplastic human tissues. Cell type-specific pattern of expression. *The Histochemical Journal*, 31(7), 433–441.
- Gantz, I., Miwa, H., Konda, Y., Shimoto, Y., Tashiro, T., Watson, S.J., DelValle, J. & Yamada, T. (1993). Molecular cloning, expression, and gene localization of a fourth melanocortin receptor. *Journal of Biological Chemistry*, 268(20), 15174–15179.
- Garay-Rojas, E., Harper, M., Hraba-Renevey, S. & Kress, M. (1996). An apparent autocrine mechanism amplifies the dexamethasone- and retinoic acid-induced expression of mouse lipocalin-encoding gene *24p3*. *Gene*, 170(2), 173–180.
- Geurts, M.H, Borsboom, D. & Ruzzano, L. (2015) Repetitive behaviors in autism and obsessive–compulsive disorder: New perspectives from a network analysis. *Journal of Autism and Developmental Disorders*, 45(1), 192–202.
- Gibb, R. & Kolb, B. (1998). A method for vibratome sectioning of Golgi–Cox stained whole rat brain. *Journal of Neuroscience Methods*, 79(1), 1–4.
- Gillan, C.M & Robbins, T.W. (2014). Goal-directed learning and obsessive–compulsive disorder. *Philosophical Transactions of the Royal Society of London: Biological Sciences*, 369(1655), 1–11.
- Gillan, C.M., Robbins, T.W., Sahakian, B.J., van den Heuvel, O.A. & van Wingen, G. (2016). The role of habit in compulsivity. *European Neuropsychopharmacology*, 26(5), 828–840.
- Glaser, E.M. & Van der Loos, H. (1981). Analysis of thick brain sections by obverse–reverse computer microscopy: Application of a new, high clarity Golgi–Nissl stain. *Journal of Neuroscience Methods*, 4(2), 117–125.
- Goetz, D.H., Holmes, M.A., Borregaard, N., Bluhm, M.E., Raymond, K.N. & Strong, R.K., (2002). The neutrophil lipocalin NGAL is a bacteriostatic agent that interferes with siderophore-mediated iron acquisition. *Molecular Cell*, 10(2), 1033–1043.
- Grados, M., Sung, H.M., Kim, S. & Srivastava, S. (2014). Genetic findings in obsessive-compulsive disorder connect to brain-derived neutrophilic factor and mammalian target of rapamycin pathways: Implications for drug development. *Drug Development Research*, 75(6), 372–383.
- Graybiel, A.M. & Grafton, S.T. (2015). The striatum: Where skills and habits meet. *Cold Spring Harbor Perspectives in Biology*, 7(8), 1–13.
- Guo, H., Jin, D. & Chen, X. (2014). Lipocalin-2 is a regulator of macrophage polarization

- and NF- $\kappa$ B/STAT3 pathway activation. *Molecular Endocrinology*, 28(10), 1616–1628.
- Guo, H., Jin, D., Zhang, Y., Wright, W., Bazuine, M., Brockman, D.A., Bernlohr, D.A. & Chen, X. (2010). Lipocalin-2 deficiency impairs thermogenesis and potentiates diet-induced insulin resistance in mice. *Diabetes*, 59(6), 1376-1385.
- Gustine, B.D.L. & Zimmermant, E.F. (1973). Developmental Changes in microheterogeneity of foetal plasma glycoproteins of mice, 132(3), 541–551.
- Harkin, B. & Kessler, K. (2011). The role of working memory in compulsive checking and OCD: A systematic classification of 58 experimental findings. *Clinical Psychology Review*, 31(6), 1004–1021.
- Hilario, M., Holloway, T., Jin, X. & Costa, R.M. (2013). Different dorsal striatum circuits mediate action discrimination and action generalization. *European Journal of Neuroscience*, 31(9), 1105–1114.
- Hilario, M. & Costa, R.M. (2007). High on habits. *Frontiers in Neuroscience*, 2(2), 208–217.
- Holmes, M.A., Paulsene, W., Jide, X., Ratledge, C. & Strong, R.K. (2005). Siderocalin (LCN2) also binds carboxymycobactins, potentially defending against mycobacterial infections through iron sequestration. *Structure*, 13(1), 29–41.
- Hraba-Renevey, S., Turler, H., Kress, M., Salomon, C. & Weil, R. (1989). SV40-induced expression of mouse gene *24p3* involves a post-transcriptional mechanism. *Oncogene*, 4(5), 601–608.
- Hvidberg, V., Jacobsen, C., Strong, R.K., Cowland, J.B., Moestrup, S.K. & Borregaard, N. (2005). The endocytic receptor megalin binds the iron transporting neutrophil-gelatinase-associated lipocalin with high affinity and mediates its cellular uptake. *FEBS Letters*, 579(3), 773–777.
- Jiang, W., Constante, M. & Santos, MM. (2008). Anemia upregulates lipocalin-2 in the liver and serum. *Blood Cells, Molecules, and Diseases*, 41(2), 169–174.
- Jin, M., Kim, J.H., Jang, E., Lee, Y.M., Soo Han, H., Woo, D.K., Park, D.H., Kook, H. & Suk, K. (2014). Lipocalin-2 deficiency attenuates neuroinflammation and brain injury after transient middle cerebral artery occlusion in mice. *Journal of Cerebral Blood Flow and Metabolism*, 34(8), 1306–1314.
- Jung, M., Mertens, C., Bauer, R., Rehwald, C. & Brüne, B. (2017). Lipocalin-2 and iron trafficking in the tumor microenvironment. *Pharmacological Research*, 120, 146–156.
- Kim, A. & Nemeth, E. (2015). New insights into iron regulation and erythropoiesis. *Current Opinion in Hematology*, 22(3), 199–205.

- Kjeldsen, L., Cowland, J. B. & Borregaard, N. (2000). Human neutrophil gelatinase-associated lipocalin and homologous proteins in rat and mouse. *Biochimica et Biophysica Acta- Protein Structure and Molecular Enzymology*, 1482(1), 272–283.
- Kjeldsen, L., Johnsen, A.H., Sengelov, H. & Borregaard, N. (1993). Isolation and primary structure of NGAL, a novel protein associated with human neutrophil gelatinase. *The Journal of Biological Chemistry*, 268(14), 10425–10432.
- Koch, J. & Exner, C. (2015). Selective attention deficits in obsessive-compulsive disorder: The role of metacognitive processes. *Psychiatry Research*, 225(3), 550–555.
- Kreitzer, A.C. (2009). Physiology and Pharmacology of Striatal Neurons. *Annual Review of Neuroscience*, 32(1), 127–147.
- Kreitzer, A.C. & Malenka, R.C. (2008). Striatal plasticity and basal ganglia circuit function. *Neuron*, 60(4), 543–554.
- Law, I.K.M., Xu, A., Lam, K.S.L., Berger, T., Mak, T.W., Vanhoutte, P.M., Law, I.K., Liu, J.T., Sweeney, G., Zhou, M.Y. & Wang, Y. (2010). Lipocalin-2 deficiency attenuates insulin resistance associated with aging and obesity. *Diabetes*, 59(4), 872–882.
- Li, Z.X., Liu, B.W., He, Z.G. & Xiang, H.B. (2017). Melanocortin-4 receptor regulation of pain. *Biochimica et Biophysica Acta - Molecular Basis of Disease*, 1863(10), 2515-2522.
- Li, H., Feng, D., Cai, Y., Liu, Y., Xu, M., Xiang, X., Zhou, Z., Xia, Q., Kaplan, M.J., Kong, X. & Gao, B. (2018). Hepatocytes and neutrophils cooperatively suppress bacterial infection by differentially regulating lipocalin-2 and NETs. *Hepatology*, 10(4), (Epub ahead of print).
- Liljeholm, M. & O’Doherty, J.P. (2012). Contributions of the striatum to learning, motivation, and performance: An associative account. *Trends Cognitive Science*, 16(9), 467–475
- Lim, S.M., Chen, D., Teo, H., Roos, A., Jansson, A.E., Nyman, T., Trésaugues, L., Pervushin, K. & Nordlund, P. (2013). Structural and dynamic insights into substrate binding and catalysis of human lipocalin prostaglandin-D synthase. *Journal of Lipid Research*, 54(6), 1630–1643.
- Lim, S.A.O., Kang, U.J. & McGehee, D.S. (2014). Striatal cholinergic interneuron regulation and circuit effects. *Frontiers in Synaptic Neurosciene*, 6(22), 1-23.
- Lim, S.K., Huang, K.W., Grueter, B.A., Rothwell, P.E & Malenka, R. C. (2012). Anhedonia requires MC4 receptor-mediated synaptic adaptations in nucleus accumbens. *Nature*, 489(1), 183–189.
- Liu, Q. & Nilsen-Hamilton, M. (1995). Identification of a new acute phase protein. *Jornal of Biological Chemistry*, 270(38), 22565–22570.

- Mallbris, L., O'Brien, K.P., Hulthen, A., Sandstedt, B., Cowland, J.B., Borregaard, N. & Stahle-Backdahl, M. (2002). Neutrophil gelatinase-associated lipocalin is a marker for dysregulated keratinocyte differentiation in human skin. *Experimental Dermatology*, 11(6), 584–591.
- Marques, F., Mesquita, S.D., Sousa, J.C., Coppola, G., Gao, F., Geschwind, D.H., Columba-Cabezas, S., Aloisi, F., Degn, M., Cerqueira, J.J., Sousa, N., Correia-Neves, M & Palha, J.A. (2012). Lipocalin-2 is present in the EAE brain and is modulated by natalizumab. *Frontiers in Cellular Neuroscience*, 6(33), 2-10.
- Marques, F., Rodrigues, A.J., Sousa, J.C., Coppola, G., Geschwind, D.H., Sousa, N., Correia-Neves, M. & Palha, J.A. (2008). Lipocalin-2 is a choroid plexus acute-phase protein. *Journal of Cerebral Blood Flow & Metabolism*, 28(3), 450–455.
- MacManus, J.P., Graber, T., Luebbert, C., Preston, E., Rasquinha, I., Smith, B. & Webster, J. (2004). Translation-state analysis of gene expression in mouse brain after focal ischemia. *Journal of Cerebral Blood Flow and Metabolism*, 24(1), 657-667.
- Meheus, L.A., Fransen, L.M., Raymackers, J.G., Block, H.A., Van Beeumen, J.J., Van Bun, S.M., Van de Voorde, A. (1993). Identification by microsequencing of lipopolysaccharide-induced proteins secreted by mouse macrophages. *The Journal of Immunology*, 151(3), 1535–1547.
- Mesquita, S.D., Ferreira, A.C., Falcao, A.M., Sousa, J.C., Oliveira, T.G., Correia-Neves, M., Sousa, N., Marques, F. & Palha, J.A. (2014). Lipocalin-2 modulates the cellular response to amyloid beta. *Cell Death and Differentiation*, 21(10), 1588–1599.
- Miethke, M. & Marahiel, M.A. (2007). Siderophore-based iron acquisition and pathogen control. *Microbiology and Molecular Biology Reviews*, 71(3), 413–451.
- Li., B. & Mody, M. (2016) Cortico-Striato-Thalamo-Cortical Circuitry, working memory, and obsessive–compulsive disorder. *Frontiers in Psychiatry*, 7(78), 1-3.
- Marcotte, E.M. (2013). Insights into the regulation of protein abundance from proteomic and transcriptomic analyses. *Nature Review Genetics*, 13(4), 227-232.
- Moreira, P.S., Marques, P., Soriano-Mas, C., Magalhães, R., Sousa, N., Soares, J.M., & Morgado, P. (2017). The neural correlates of obsessive-compulsive disorder: A multimodal perspective. *Translational Psychiatry*, 7(8), 1116-1224.
- Moreno-Navarrete, J.M., Ortega, F., Rodríguez, A., Latorre, J., Becerril, S., Sabater-Masdeu, M., Ricart, W., Frühbeck, G., Fernández-Real, J. M. & Fernández-Real, J.M. (2017). HMOX1 as a marker of iron excess-induced adipose tissue dysfunction, affecting glucose uptake and respiratory capacity in human adipocytes. *Diabetologia*, 60(5), 915–926.
- Moschen, A.R., Gerner, R.R., Wang, J., Klepsch, V., Adolph, T.E., Reider, S.J., Hackl,

- H., Pfister, A., Schilling, J., Moser, P.L., Kempster, S.L., Swidsinski, A., Höller, D., Weiss, G., Baines, J.F., Kaser, A. & Tilg, H. (2016). Lipocalin-2 protects from inflammation and tumorigenesis associated with gut microbiota alterations. *Cell Host and Microbe*, 19(4), 455–469.
- Mosialou, I., Shikhel, S., Liu, J.M., Maurizi, A., Luo, N., He, Z., Huang, Y., Zong, H., Friedman, R.A., Barasch, J., Lanzano, P., Deng, L., Leibel, R.L., Rubin, M., Nickolas, T., Chung, W., Zeltser, L.M., Williams, K.W., Pessin, J.E. & Kousteni, S. (2017). MC4R-dependent suppression of appetite by bone-derived lipocalin 2. *Nature*, 543(7645), 385–390.
- Mucha, M., Skrzypiec, A.E., Schiavon, E., Attwood, B.K., Kucerova, E. & Pawlak, R. (2011). Lipocalin-2 controls neuronal excitability and anxiety by regulating dendritic spine formation and maturation. *Proceedings of the National Academy of Sciences*, 108(45), 18436–18441.
- Nairz, M., Theurl, I., Schroll, A., Theurl, M., Fritsche, G., Lindner, E., Seifert, M., Crouch, M. L., Hantke, K., Akira, S., Fang, F.C. & Weiss, G. (2009). Absence of functional Hfe protects mice from invasive *Salmonella enterica* Serovar *Typhimurium* infection via induction of lipocalin-2. *Blood*, 114(17), 3642–3651.
- Neilands, J.B. (1995). Siderophores : Structure and function of microbial iron transport compounds. *The Journal of Biological Chemistry*, 270(45), 26723–26726.
- Nestadt, G., Grados, M. & Samuels, J. (2011). Genetics of OCD. *Psychiatric Clinics of North America*, 33(1), 1–17.
- Nicholson, L.B. (2016). The immune system. *Essays In Biochemistry*, 60(3), 275–301.
- Njung'e, K. & Handley, S.L. (1991). Effects of 5-HT uptake inhibitors, agonists and antagonists on the burying of harmless objects by mice; a putative test for anxiolytic agents. *British Journal of Pharmacology*, 104(1), 105–112.
- Nopoulos, P.C. (2016). Huntington disease: A single-gene degenerative disorder of the striatum. *Dialogues in Clinical Neuroscience*, 18(1), 91–98.
- Owen, H.C., Roberts, S.J., Ahmed, S.F. & Farquharson, C. (2008) Dexamethasone-induced expression of the glucocorticoid response gene lipocalin-2 in chondrocytes. *American Journal of Physiology- Endocrinology and Metabolism*, 294(1), 1023-1034
- Pandit, R., Van Der Zwaal, E.M., Luijendijk, M.C.M., Brans, M.A.D., Van Rozen, A.J., Ophuis, R.J.A.O., Vanderschuren, L.J.M.J., Adan, R.A.H & Fleur, S.E. (2015). Central melanocortins regulate the motivation for sucrose reward. *PLoS ONE*, 10(3), 1–15.
- Parmar, A. & Sarkar, S. (2016). Neuroimaging studies in obsessive-compulsive disorder: A narrative review. *Indian Journal of Psychological Medicine*, 38(5), 386–394.
- Parrow, N.L., Fleming, R.E. & Minnick, M.F. (2013). Sequestration and scavenging of

- iron in infection. *Infection and Immunity*, 81(10), 3503–3514.
- Pauls, D.L., Abramovitch, A., Rauch, S.L. & Geller, D.A. (2014). Obsessive–compulsive disorder: An integrative genetic and neurobiological perspective. *Nature Reviews Neuroscience*, 15(6), 410–424.
- Peça, J., Feliciano, C., Ting, J.T., Wang, W., Wells, M.F., Venkatraman, T.N., Lascola, C.D., Fu, Z. & Feng, G. (2011). *Shank3* mutant mice display autistic-like behaviours and striatal dysfunction. *Nature*, 472(7344), 437–442.
- Piantadosi, S.C. & Ahmari, S.E. (2015). Using optogenetics to dissect the neural circuits underlying OCD and related disorders. *Current Treatment Options in Psychiatry*, 2(3), 297–311.
- Poh, K.W., Yeo, J.F., Stohler, C.S. & Ong, W.Y. (2012). Comprehensive gene expression profiling in the prefrontal cortex links immune activation and neutrophil infiltration to antinociception. *Journal of Neuroscience*, 32(1), 35–45.
- Porritt, M.J., Batchelor, P.E., Hughes, A.J., Kalnins, R., Donnan, G.A. & Howells, D.W. (2000). New dopaminergic neurons in Parkinson’s disease striatum. *Lancet*, 356(9223), 44–45.
- Radley, J.J., Sisti, H.M., Hao, J., Rocher, A.B., McCall, T., Hof, P. R. & Morrison, J.H. (2004). Chronic behavioral stress induces apical dendritic reorganization in pyramidal neurons of the medial prefrontal cortex. *Neuroscience*, 125(1), 1–6.
- Robertson, M.M., Eapen, V., Singer, H.S., Martino, D., Scharf, J. M., Paschou, P., Veit Roessner, V., Woods, D.W., Hariz, M., Mathews, C.A., Črnčec, R. & Leckman, J.F. (2017). Gilles de la Tourette syndrome. *Nature Reviews Disease Primers*, 3(1), 7–16.
- Rosario-Campos, M.C., Miguel, E.C., Quatrano, S., Chacon, P., Ferrao, Y., Findley, D. & Leckman, J.F. (2006). The dimensional Yale-Brown Obsessive-Compulsive Scale (dY-BOCS): An instrument for assessing obsessive-compulsive symptom dimensions. *Molecular Psychiatry*, 11(5), 495–504.
- Saito, H. (2014). Metabolism of iron. *Journal of the American Medical Association*, 115(12), 1039–1051.
- Savage, C.R., Baer, L., Keuthen, N.J., Brown, H.D., Rauch, S.L. & Jenike, M.A. (1999). Organizational strategies mediate nonverbal memory impairment in obsessive-compulsive disorder. *Biological Psychiatry*, 45(7), 905–916.
- Saxena, S. & Rauch, S.L. (2000). Functional neuroimaging and the neuroanatomy of obsessive-compulsive disorder. *Psychiatric Clinics of North America*, 23(3), 563–586.
- Schroll, A., Eller, K., Feistritz, C., Nairz, M., Sonnweber, T., Moser, P.A. & Weiss, G. (2012). Lipocalin-2 ameliorates granulocyte functionality. *European Journal of*



- Immunology*, 42(12), 3346–3357.
- Sholl, D.A. (1956). The measurable parameters of the cerebral cortex and their significance in its organization. *Progress in Neurobiology*, 324–333.
- Snyder, H.R., Kaiser, R.H., Warren, S.L., Heller, W., Hall, F. & Hospital, M. (2015). Obsessive-compulsive disorder is associated with broad impairments in executive function: A meta-analysis. *Clinical Psychological Science*, 3(2), 301–330.
- Tepper, J.M., Koós, T. & Wilson, C.J. (2004). GABAergic microcircuits in the neostriatum. *Trends in Neurosciences*, 27(11), 662–669.
- Tomczak, M. & Tomczak, E. The need to report effect size estimates revisited. An overview of some recommended measures of effect size. *Trends in Sport Sciences*, 1(21), 2299-9590.
- Triebel, S., Bläser, J., Reinke, H. & Tschesche, H. (1992). A 25 kDa  $\alpha$ 2-microglobulin-related protein is a component of the 125 kDa form of human gelatinase. *FEBS Letters*, 314(3), 386–388.
- Uylings, H.B.M., Ruiz-Marcos, A. & van Pelt, J. (1986). The metric analysis of three-dimensional dendritic tree patterns: A methodological review. *Journal of Neuroscience Methods*, 18(2), 127–151.
- Voorn, P., Vanderschuren, L.J.M.J., Groenewegen, H.J., Robbins, T.W. & Pennartz, C.M.A. (2004). Putting a spin on the dorsal-ventral divide of the striatum. *Trends in Neurosciences*, 27(8), 468–474.
- Wan, Y., Ade, K.K., Caffall, Z., Ozlu, M., Eroglu, C., Feng, G. & Calakos, N. (2014). Circuit-selective striatal synaptic dysfunction in the *sapap3* knockout mouse model of obsessive-compulsive disorder. *Biological Psychiatry*, 75(8), 623–630.
- Welch, M., Lu, J., Rodriguiz, R.M., Trotta, N.C., Peca, J., Ding, J.D. & Feng, G. (2007). Cortico-striatal synaptic defects and OCD-like behaviours in Sapap3-mutant mice. *Nature*, 448(7156), 894–900.
- Xing, C., Wang, X., Cheng, C., Montaner, J., Mandeville, E., Leung, W., van Leyen K., Lok, J., Wang, X. & Lo, E.H. (2014). Neuronal production of lipocalin-2 as a help-me signal for glial activation. *Stroke*, 45(9), 2085–2092.
- Xu, G., Ahn, J.H., Chang, S.Y., Eguchi, M., Ogier, A., Han, S.J. & Sweeney, G. (2012). Lipocalin-2 induces cardiomyocyte apoptosis by increasing intracellular iron accumulation. *Journal of Biological Chemistry*, 287(7), 4808–4817.
- Xu, P., Grueter, B.A., Britt, J. K., McDaniel, L., Huntington, P.J., Hodge, R. & Pieper, A.A. (2013). Double deletion of melanocortin 4 receptors and SAPAP3 corrects compulsive behavior and obesity in mice. *Proceedings of the National Academy of Sciences*, 110(26), 10759–10764.
- Yan, Q., Yang, Q., Mody, N., Graham, T.E., Hsu, C., Xu, Z. & Rosen, E.D. (2007). The

- adipokine lipocalin-2 is regulated by obesity and promotes insulin resistance. *October*, 56(1), 2533–2540.
- Yang, J., Bielenberg, D.R., Rodig, S.J., Doiron, R., Clifton, M. C., Kung, A.L. & Moses, M.A. (2009). Lipocalin-2 promotes breast cancer progression. *Proceedings of the National Academy of Sciences USA*, 106(10), 3913–3918.
- Yang, J., Goetz, D., Li, J.Y., Wang, W., Mori, K., Setlik, D. & Barasch, J. (2002). An iron delivery pathway mediated by a lipocalin. *Molecular Cell*, 10(5), 1045–1056.
- Yien, Y.Y. & Paw, B.H. (2016). A role for iron deficiency in dopaminergic neurodegeneration. *Proceedings of the National Academy of Sciences*, 113(13), 3417–3418.
- Yin, H.H., Ostlund, S.B., Knowlton, B.J. & Balleine, B.W. (2005). The role of the dorsomedial striatum in instrumental conditioning. *European Journal of Neuroscience*, 22(2), 513–523.
- Yun, J.Y., Jang, J.H., Jung, W.H., Shin, N.Y., Kim, S.N., Hwang, J.Y. & Kwon, J.S. (2017). Executive dysfunction in obsessive-compulsive disorder and anterior cingulate-based resting state functional connectivity. *Psychiatry Investigation*, 14(3), 333-343.
- Chan, R.Y., Liu, J.S., Pociask, D.A., Zheng, M., Mietzner, T.A., Berger, T., Mak, T.W., Clifton, M.C., Strong, R.K., Ray, P. & Kools, J.K. (2009). Lipocalin-2 is required for pulmonary host defense against *Klebsiella* infection. *The Journal of Immunology*, 15(8), 4947–4956.
- Zhang, J., Wu, Y., Zhang, Y., LeRoith, D., Bernlohr, D.A. & Chen, X. (2008). The role of lipocalin-2 in the regulation of inflammation in adipocytes and macrophages. *Molecular Endocrinology*, 22(6), 1416–1426.
- Zhang, Y., Foncea, R., Deis, J.A., Guo, H., Bernlohr, D.A. & Chen, X. (2014). Lipocalin-2 expression and secretion is highly regulated by metabolic stress, cytokines, and nutrients in adipocytes. *PLoS ONE*, 9(5), 1–9